Plant genome response to incoming coding sequences: stochastic transcriptional activation independent of integration loci

Soichirou Satoh[1¶], Takayuki Hata[1,2¶], Naoto Takada[1], Makoto Tachikawa[1], Mitsuhiro Matsuo[2], Sergei Kushnir[3], and Junichi Obokata[2]*

[1] Graduate School of Life and Environmental Sciences, Kyoto Prefectural University, Kyoto-shi, Kyoto, Japan

[2] Faculty of Agriculture, Setsunan University, Hirakata-shi, Osaka, Japan

[2] Plant Molecular Genetics, Teagasc, Crop Science Department, Oak Park, Ireland

* Corresponding author

Email: junichi.obokata@setsunan.ac.jp

[¶] These authors contributed equally to this work.

Soichirou Satoh and Takayuki Hata should be considered joint first author.

Abstract

Horizontal gene transfer can occur between phylogenetically distant organisms, such as prokaryotes and eukaryotes. In these cases, how do the translocated genes acquire transcriptional competency in the alien eukaryotic genome? According to the conventional view, specific loci of the eukaryotic genome are thought to provide transcriptional competency to the incoming coding sequences. To examine this possibility, we randomly introduced the promoterless luciferase (LUC)-coding sequences into the genome of *Arabidopsis thaliana* cultured cells and performed a genome-wide "transgene location vs. expression" scan. We mapped 4,504 promoterless *LUC* inserts on the *A. thaliana* chromosomes, and found that about 30% of them were transcribed. Only a small portion of them were explained by the conventional transcriptional fusions with the annotated genes, and the remainder occurred in a quite different manner; (1) they occurred all over the chromosomal regions, (2) independently of the insertion sites relative to the annotated gene loci, inherent transcribed regions, or heterochromatic regions, and (3) with one magnitude lower transcriptional level than the conventional transcriptional fusions. This type of transcriptional activation occurred at about 30% of the inserts, raising a question as to what this 30% means. We tested two hypotheses: the activation occurred at 30% of the entire chromosomal regions, or stochastically at 30% of each insertion event. Our experimental analysis indicates that the latter model could explain this transcriptional activation, a new type of plant genome response to the incoming coding sequences. We discuss the possible mechanisms and evolutionary roles of this phenomenon in the plant genome.

Introduction

Horizontal or endosymbiotic gene transfer (HGT/EGT) events greatly contributed to the evolution and diversification of terrestrial life and organisms [1, 2]. In the plant phyla, thousands of genes originally encoded by photosynthetic bacteria were transferred to the host nuclear genome to produce photosynthetic eukaryotes [3], even though the bacterial genome systems were quite different from those of eukaryotes. The genetic flow from the plastid to the nuclear genome is ongoing [4, 5].

However, the mechanisms by which foreign genes obtained by HGT/EGT events acquired transcriptional competency in the host nuclear genome remain largely unclear. Examination of the transferred DNA fragments from the plastid to the nucleus led to the proposal that the translocated genes were transcribed as fusion transcripts via trapping of endogenous genes/promoters [6, 7]. This transcriptional activation mechanism is easy to understand, but one promoter-acquisition event will result in one disruption of a preexisting gene. Therefore, it has a shortcoming with regard to explaining the thousands of functional gene transfers that occurred in the endosymbiotic evolution.

The cryptic promoter hypothesis could be an alternative to explain the transcriptional activation of exogenously incoming genes in the nucleus. This hypothesis was originally adopted to explain the enigmatic expression of the coding sequences in gene-/promoter-trapping experiments; promoterless coding sequences were occasionally transcribed without obvious trapping of any annotated genes/promoters [8–14]. The cryptic promoter hypothesis postulated that the invisible promoters hidden in the genome, namely cryptic promoters, capture the incoming coding sequences to cause their detectable transcription. However, molecular identities of these cryptic promoters have long been unsolved. Recently, we demonstrated that such unexpected transcriptional activation in gene-/promoter-trapping experiments occurred via at least two different mechanisms in the plant genome: (1) cryptic promoter capturing, in which exogenous DNA was transcribed by trapping a preexisting promoter-like chromatin configuration that is not associating with annotated genes; and (2) promoter *de novo* origination, in which promoter-like epigenetic landscapes were newly formed via chromatin remodeling triggered by the insertion of a coding sequence [15]. We should note that these two mechanisms could endow transcriptional activity to the incoming coding sequences without disturbing the preexisting nuclear gene network. In examining whether these cryptic promoters could be a source of transcriptional activation in massive gene transfer, we should know how often the cryptic promoter activation occurs in the whole nuclear genome.

In this study, we applied a massively parallel reporter assay [16, 17] to the conventional gene-/promoter-trapping experiments and carried out a genome-wide “transgene location vs. expression” scan. We introduced thousands of promoterless coding sequences of firefly

78 luciferase (LUC) genes as a model of transferred genes into the genome of *Arabidopsis*
79 *thaliana* cultured cells, and examined the manners by which transcriptionally inert transgenes
80 become activated in the foreign genome environment. We found that a small portion of the
81 transcriptional activation of transgenes was explained by the conventional gene-/promoter-
82 trapping mechanism, but the majority of promoterless *LUC* inserts were transcriptionally
83 activated in a quite different manner, i.e., integration-dependent stochastic transcriptional
84 activation. This transcriptional activation occurred stochastically at about 30% of each insertion
85 event, independently of the integration locus relative to the preexisting genes, inherent
86 transcribed regions, or heterochromatic regions. We discuss the likely mechanism of this
87 transgene activation phenomenon and refer to its possible contribution to the initial
88 transcriptional activation process of HGT/EGT during plant genome evolution.

89

90 # Results

91 **General view of the transgene expression over the entire genome**

92 To understand the rules that govern the transcriptional activation of alien incoming genes, we
93 introduced thousands of promoterless luciferase (*LUC*) genes into *A. thaliana* T87 suspension-
94 cultured cells via *Agrobacterium*-mediated transformation (S1A Fig). In the pools of transformed
95 cells, 4,504 *LUC* genes were mapped onto the *A. thaliana* genome (Fig 1A, and S1B, C, and S2
96 Figs). The *LUC* genes were evenly distributed across the length of the five *A. thaliana*
97 chromosomes, with the exception of the pericentromeric regions, where the insertion frequency
98 was significantly lower (Fig 1A). The relative abundances of the *LUC* genes inserted in the
99 intergenic, genic, and promoter regions were roughly proportional to the relative lengths of
100 these genomic regions (Fig 1B and S3 Fig). On the fine distribution map of the inserts, genic
101 promoter regions (~200 bp) were more prone to be inserted than the other regions by about
102 threefold (Fig 1B, and S3 and S4 Figs), in accordance with a relatively open chromatin
103 configuration of the promoter region. Despite such slight biases, the *LUC*-mapped loci covered
104 entire chromosomal regions (Fig 1A and B), and thus were suitable for the genome-wide
105 scanning of transgene transcriptional activation events.

106 RNA deep sequencing was used to detect and measure the *LUC* expressions. Unique
107 barcode identifiers enabled us to link the distinct genomic locations and *LUC* transcription levels
108 at each position (Fig 1, and S1B and D Fig). We found that 1,355 of the 4,504 *LUC* genes
109 identified were transcribed with a ~10^5-fold variation in *LUC* mRNA levels (Fig 1D). Some
110 barcodes could possibly behave as *cis*-regulatory elements and affect their own expression.
111 However, our correlation analyses did not provide evidence of such function of barcode
112 sequences (S5 and S6 Figs).

113 **Identification of two distinct mechanisms of transgene transcriptional activation**

114 In the simplest-case scenario, promoterless *LUC* transcription is a result of the trapping of
115 endogenous transcription units. To test this conventional model, we classified the 4,504 *LUC*
116 loci into five insertion types in relation to the annotated genes: (i) sense and (ii) antisense
117 orientation within the gene-coding regions, (iii) sense and (iv) antisense orientation in the
118 promoter regions, and (v) intergenic regions. According to this classification, 25–30% of the
119 *LUC* genes in each insertion type were transcribed, except for the genic-sense insertion type;
120 about 50% of them were transcribed in the genic-sense fraction (Fig 1C). Why are the genic-
121 sense inserts more prone to be transcribed?

122 As shown in Fig 1D, the transcription levels of *LUC* genes in each insertion type ranged from
123 10^1 to 10^7 at the mean transcription level of 10^4, with that of the genic sense type exceptionally
124 high, at the level of 10^5. The comparison of the distribution profiles of the five insertion types
125 revealed that the genic-sense type had a superposed fraction (light-blue fraction in Fig 1D) at
126 higher transcription levels (10^5–10^7). Without this superposed fraction, the distribution curves of
127 the five *LUC* insertion types were remarkably similar (Fig 1D). To explain this result, we next
128 examined the *LUC* insertion sites relative to the annotated genic transcription start sites (TSSs)
129 and *LUC* transcription levels (Fig 1E). We found that the *LUC* inserts with higher transcription
130 levels (10^5–10^7) were more abundant at 0.2–2.4 kb downstream of the annotated TSSs (Fig 1E).
131 Without this superposed fraction in this region, the expressed inserts appeared to be similarly
132 distributed both within and outside of the annotated transcribed regions (S7 Fig). In *A. thaliana*,
133 the median lengths of the 5′ untranslated regions (UTRs) and mRNAs are ~70 and ~1,900 bp,
134 respectively (as calculated from the TAIR10 database, https://www.arabidopsis.org/index.jsp);

135 thus, the region 0.2–2.4 kb downstream from the annotated TSS roughly corresponds to the
136 intrinsic protein-coding regions. Based on these observations, the *LUC* inserts of the genic-
137 sense type appeared to be transcribed at least in part by the conventional gene-trapping
138 mechanism, in addition to the transgene transcription mechanism that similarly occurred over
139 the entire genome.

140 If our above assumption is the case, the contribution of the conventional gene-trapping to
141 the whole transcriptional activation of the incoming coding sequences is small; rather, the
142 majority of transcriptional activation occurred by the distinct mechanism, even within the genic-
143 sense insertion type (Fig 1D–F). The mean transcription level of this transcriptional activation
144 was 10^4, which was one magnitude lower than that of the conventional transcriptional fusions
145 (Fig 1D and E). To confirm that this whole expression profile was not a sequencing artifact, we
146 performed similar analyses using more reliable datasets (i.e., the *LUC* inserts whose
147 sequencing reads were more highly abundant than the background level) with elevated read
148 number threshold. Irrespective of the threshold read numbers, two distinct fractions
149 corresponding to the gene-trapping type (light-blue fraction in S8A and B Fig) and the other
150 type (light-red fraction in S8A and B Fig) were clearly detected, as in Fig 1D. In addition, these
151 distribution profiles were confirmed by three biologically independent samples (S8C–E Fig).
152 Based on these analyses, we concluded that the low-level transcriptional activation of
153 transgenes that occurred over the entire chromosomal regions was not a sequencing artifact.

154 **Promoterless *LUC* genes were transcribed regardless of inherent transcriptional**
155 **activities**

156 Pervasive transcription throughout the genome characterizes eukaryotic organisms. We asked
157 whether the genome-wide transcription of the *LUC* genes could be explained by the integration
158 within such pervasively transcribed regions. To define the genomic transcription landscape of
159 the *A. thaliana* T87 cells studied here, we performed deep RNA sequencing of the wild-type
160 (WT) cells. We classified the 4,504 *LUC* loci by comparing their transcription status between
161 transgenic and WT cells (Fig 2A). Unexpectedly, only 7.8% of the *LUC* genes were transcribed
162 in the inherently transcribed genomic regions (type (iii) in Fig 2A), whereas 22.3% of the *LUC*
163 genes were transcribed in the transcriptionally inert regions (type (i) in Fig 2A). As for the 7.8%

164 of the *LUC* genes (type (iii) in Fig 2A), we compared the transcription levels between the
165 transgenic and WT cells, but no correlation was found (Fig 2B, $r = 0.21$). Two conclusions were
166 drawn from this analysis: (1) transcriptional activation of the *LUC* inserts occurs independently
167 of the inherent transcriptional status of the genomic region where the *LUC* was inserted; and (2)
168 the transcriptional activities of the *LUC* inserts do not reflect the inherent transcriptional
169 activities of the given genomic regions.

170 **Transcriptional activation of promoterless *LUC* genes was not affected by the inherent**
171 **heterochromatic status**

172 We wondered whether *LUC* transgenes could overcome the silencing effects of the histone
173 code. In *A. thaliana*, the dimethylation of the ninth lysine residue of histone H3 (H3K9me2) is
174 thought to be associated with transcriptional silencing in the heterochromatic regions [18–20]. A
175 Chromatin immunoprecipitation-sequencing (ChIP-Seq) analysis of the WT *A. thaliana* T87 cells
176 revealed that 15.6% of the genome was covered by H3K9me2-containing chromatin and was
177 largely associated with pericentromeric regions. In the transgenic cells, only 120 *LUC* genes
178 were inserted into the H3K9me2-containing heterochromatic regions (see the legend of Fig 3),
179 indicating that the integration frequency in this region was one-seventh of the rest of the
180 genome. However, in the H3K9me2-containing region, 28% of the *LUC* inserts were
181 transcriptionally activated and their activation profiles were similar to the other regions (Fig 3A).
182 The transcription levels of these *LUC* genes did not show any correlation with the degree of
183 H3K9me2 modification (Fig 3B). Furthermore, two transcribed *LUC* genes were located 63 kb
184 and 682 kb from the centromeres (S9 Fig), and these regions were covered by pericentromeric
185 heterochromatin [21]. Taken together, we concluded that the transcriptional activation of the
186 *LUC* inserts occurred at a rate of about 30% irrespective of the inherent heterochromatic status.

187 **Integration-dependent stochastic activation of transgene transcription**

188 As described above, transgene transcriptional activation was observed for 30% of the *LUC*
189 inserts, which raised a question: What does this 30% mean? To account for this question, we
190 hypothesized two models: (i) the transcriptional activation occurred at 30% of the entire *A.*
191 *thaliana* chromosomal regions; or (ii) stochastically at 30% of each insertion event. To test
192 which model is suitable for this transcriptional activation, we analyzed the transcriptional

193 behavior of *LUC* genes that were integrated into close neighboring locations (Fig 4A).
194 Theoretically, *LUC* pairs inserted in close proximity could result in three transcriptional fates:
195 expression of both *LUC* genes (Fate A); expression of one *LUC* gene and silencing of the other
196 (Fate B); and silencing of both *LUC* genes (Fate C) (Fig 4B). If the transgene transcriptional
197 activation depends on the chromosomal locus, the transcriptional fates of neighboring *LUC*
198 inserts are expected to be similar (Fig 4C). Hence, in this scenario, only Fates A and C would
199 be observed for the *LUC* pairs (Fig 4C). Moreover, the expected ratio between Fates A and C
200 would be 30:70 (Fig 4C), assuming an average transcriptional activation rate of 30%.
201 Conversely, as shown in Fig 4D, if the transgene transcriptional activation occurs stochastically
202 at 30% of each integration event and is independent of the chromosomal locus, the distribution
203 of the transcriptional fates of *LUC* pairs would fit the joint probability of two individual activation
204 events. In this model, the distribution ratio among Fates A, B, and C would be 9, 42, and 49,
205 respectively (Fig 4D). According to these expectations, we examined which activation model fits
206 the transcriptional activation of promoterless *LUC* genes. In our dataset, we identified 21
207 genomic locations in which independent *LUC* inserts were integrated within a 50-bp sliding
208 window. Among these 21 *LUC* insert pairs, all three possible transcriptional fates were
209 observed, as follows: Fate A, three cases; Fate B, five cases; and Fate C, 13 cases (Fig 4E,
210 upper panel). This distribution fits the integration-dependent stochastic transcriptional activation
211 model (Fig 4D), rather than the chromosomal-locus-dependent model (Fig 4C). In fact, the
212 expected values, i.e., Fate A (1.9 events), Fate B (8.8 events), and Fate C (10.2 events), were
213 not significantly different from the observed rates (Fisher's exact test, $P = 0.55$) (Fig 4F). To
214 perform a more rigorous test of the stochastic transcriptional activation model, we reduced the
215 sliding window to 10 bp, which yielded 12 genomic locations (Fig 4E, lower panel). Similar to
216 the results of the 50-bp sliding window analysis, the pairwise *LUC* comparison did not detect
217 significant differences (Fisher's exact test, $P = 0.82$) between the observed and theoretical
218 values (Fate A, 1.0 vs. 1.1; Fate B, 3.0 vs. 5.0; Fate C, 8.0 vs. 5.9) (Fig 4F). It should be
219 emphasized that the individual *LUC* inserts used for this integration-site neighborhood analysis
220 stemmed from different, independently transformed cells that passed through ~10 cell divisions
221 before nucleic acid extraction. Thus, we concluded that the transgene transcriptional activation

222 in a given genome location was likely to be the outcome of an integration-dependent stochastic
223 phenomenon.

224

225 Discussion

226 In this study, we performed a genome-wide screening of promoter-trapping events covering
227 both expressed and unexpressed inserts for the first time, using a non-selective reporter.
228 Collectively, the data revealed a new type of transgene transcriptional activation of the plant
229 genome, which occurs stochastically at about 30% of each DNA integration event but not
230 depending on the chromosomal loci. This transcriptional activation occurred in the transgenic
231 cells that experienced only ~10 times cell divisions after the transgene integration, indicating
232 that it is an immediate response of the plant genome to the incoming coding sequences. To
233 date, we could not find any specific motifs that were enriched at the 5′ proximal regions of the
234 transcribed *LUC* genes, which was quite a different situation from the annotated gene
235 promoters (S10 Fig). How can we explain the mechanism of this new type of transcriptional
236 activation that is stochastic and independent of the DNA sequences surrounding the transgene
237 insertion sites?

238 It is generally accepted that T-DNA is integrated into the host genome following the double-
239 stranded DNA breaks, which are repaired predominantly by the non-homologous DNA end-
240 joining [22, 23]. This repair process remodels the chromatin and leaves so-called DNA damage
241 scars in the chromatin epigenetic structure [24, 25]. This chromatin remodeling may account, at
242 least in part, for the integration-dependent stochastic transcriptional activation. From this
243 viewpoint, it is intriguing to compare the chromatin structures before and after the *LUC*
244 integration, but this analysis remains technically challenging. In the present study, the
245 established transgenic cell pools were highly heterogeneous; they contained thousands of
246 distinct transgenic cell lines, and each cell line consisted of only ~1,000 cells. There is no
247 practical methodology to analyze epigenetic configurations of each transgenic line from such a
248 heterogeneous cell population. Recently, single-molecular resolution techniques were reported
249 for the chromatin accessibility assay [26–28], but further technical breakthrough is needed to

250 determine the epigenetic marks on the single chromatin molecule. In addition, the *LUC* mRNA
251 level of each transgenic line was quite low compared with the annotated gene transcripts.
252 Therefore, TSS determination of the *LUC* inserts is also challenging. We are now attempting
253 these challenging analyses, which would provide useful information to depict the transcription
254 initiation mechanism in this new type of plant genome response.

255 In the present study, we characterized a novel plant genome response to the incoming
256 coding sequences, i.e., integration-dependent stochastic transcriptional activation. Contrary to
257 the conventional gene-/promoter-trapping scenario in the HGT/EGT process, this foreign gene
258 activation mechanism seems less harmful to the host nuclear gene networks because this
259 mechanism does not cause disruption of the preexisting nuclear genes. Therefore, this finding
260 provides a new angle for examining the gene activation mechanism in the massive gene
261 transfer events between phylogenetically distant organisms. To evaluate the biological
262 contribution of this novel genome response to plant genome evolution, further information is
263 needed on how activated transcription via this mechanism continues and behaves over
264 generations, and how selective pressure on the activated transcriptions affects their fates.
265 Experimental studies along these lines could open the way to an understanding of how the
266 initial molecular response of the eukaryotic genome is linked to the phenotypic evolution.

267 Materials and Methods

268 Construction of barcode-labelled plasmid libraries

269 The transformation vector plasmid was constructed using a modified pGreenII vector [29, 30] to
270 encode 12 bp of random sequence ("barcode"), a promoterless firefly luciferase (*luc*+) coding
271 sequence, a *nos* terminator sequence and an expression cassette of a kanamycin-resistant
272 gene within the T-DNA region (S1A Fig and S1 Methods). All primers used in this study are
273 listed in S1 Table.

274 Plant cell culture and transformation

275 *A. thaliana* T87 cells [31] were cultured in mJPL3 medium [32] under continuous illumination
276 (60 μE m^{-1} s^{-1}) at 22°C with shaking (120 rpm). One-week-old cultures were collected using a

277 10 μm nylon mesh, washed with H_2O twice and subjected to DNA, RNA and chromatin isolation
278 and transformation.

279 *Agrobacterium tumefaciens* (GV3101) cells were transformed with the barcode-labelled
280 libraries. *Agrobacterium*-mediated transformation of *A. thaliana* T87 cells was carried out
281 according to the published protocol [32, 33]. We obtained three independently transformed
282 pools of T87 cells (termed TRIP pools hereafter), which were grown on mJPL3 plates
283 containing 25 μg ml^{-1} meropenem (MEPM) and 30 μg ml^{-1} kanamycin (Km) at 22°C under
284 continuous illumination for about 2 weeks. Green calli were cultured in liquid mJPL3 medium
285 containing 12.5 μg ml^{-1} MEPM and 10 μg ml^{-1} Km with shaking under continuous illumination at
286 22°C for 2 weeks. Finally, the cells were transferred to fresh mJPL3 medium and grown for 1
287 additional week.

288 **Determination of the insertion loci of *LUC* genes**

289 Two micrograms of genomic DNA extracted from the TRIP pools using the DNeasy Plant Mini
290 Kit (QIAGEN) were digested completely with *Dpn*II, purified using the QIAquick PCR purification
291 kit (QIAGEN) and circularized with T4 DNA ligase. After purification using the QIAquick PCR
292 purification kit, the circularized DNA was subjected to inverse PCR using primers that were
293 designed to hybridize within the *LUC* gene (S1B Fig). From this point, we prepared two types of
294 sequencing libraries: (1) The inverse PCR product was digested completely with *Apa*LI or *Sca*I
295 to block the amplification of the vector-backbone-containing fragments in the subsequent steps.
296 Nested PCR was performed, followed by sequencing library preparation using the Nextera XT
297 DNA Sample Prep Kit (Illumina); (2) The inverse PCR product was subjected to tailed-PCR and
298 digestion with *Apa*LI or *Sca*I, followed by the addition of terminal adapters via one additional
299 round of PCR, to prepare the sequencing libraries essentially according to Akhtar *et al*. [16].
300 Sequencing was performed on an Illumina MiSeq sequencer with 301 bp paired-end reads.

301 The insertion loci of *LUC* genes were determined using an open-source software and
302 custom Perl scripts (S1B, and C Fig). Briefly, the sequencing reads were trimmed from the 3′
303 end with a phred-scaled quality score ≥30. Reads containing a *LUC* segment (31 bp), the
304 barcode (12 bp) and a *LUC* flanking sequence (25–50 bp) were extracted. The *LUC* flanking

305 sequences were mapped to the TAIR10 version of the *A. thaliana* genome using Bowtie [34]
306 with the following parameters; *bowtie -m 1 -v 3*. Subsequently, the 3′-junction sites of the
307 mapped flanking sequences were defined as the genomic loci of the corresponding *LUC* inserts.
308 Reliable locus–barcode pairs of *LUC* inserts were collected according to their read depth; at
309 least three reads and 90% of individual mapped loci were occupied by an identical barcode
310 sequence. We combined all *LUC* loci that were derived from three biologically independent
311 TRIP pools, as well as from two of mapping libraries, and subjected them to subsequent
312 analyses. For additional details, see S1 Methods.

313 **Determination of the relative transcription levels of *LUC* genes**

314 RNA was extracted from the TRIP pool using the RNeasy Plant Mini Kit (QIAGEN) and treated
315 with RNase-free DNase I (QIAGEN). cDNA was synthesized from 5 μg of the RNA using an
316 oligo dT_{15} primer and SuperScript III Reverse Transcriptase (Thermo Fisher Scientific).
317 Sequencing libraries were prepared by amplification of the barcode region using primers with
318 an adapter extension, followed by tailed-PCR using Nextera XT Index Primers (Illumina) (S1B
319 Fig). From an aliquot of DNA from the TRIP pools, sequencing libraries of the barcode region
320 were prepared using the method described above. These cDNA and DNA libraries were
321 sequenced on an Illumina MiSeq sequencer with 76 bp paired-end reads.

322 To determine the relative transcription levels of *LUC* genes, barcode sequences were
323 extracted from sequencing reads and counted. Barcode sequences with a read number ≤5 in
324 the DNA library were omitted. Moreover, barcode sequences with a read number ≤5 in the
325 cDNA library were set as zero. For each library, the read number of each barcode was
326 normalized to the total reads of the library. To obtain an indicator of the RNA level per DNA
327 molecule, the cDNA read number was divided by the corresponding DNA read number and
328 multiplied by 10,000, which was used to indicate the transcription levels of the individual *LUC*
329 genes. For additional details, see S1 Methods.

330 **RNA-Seq**

331 RNA was extracted using the RNeasy Plant Mini Kit (QIAGEN) and treated with RNase-free
332 DNase I (QIAGEN). RNA-Seq libraries were prepared using the SureSelect Strand-Specific

333 RNA-Seq Kit (Agilent), according to the manufacturer's instructions. The libraries were
334 sequenced on an Illumina MiSeq sequencer with 76 bp paired-end reads. The sequencing
335 reads from two replicated experiments were combined. The transcribed regions and their
336 expression levels were determined using STAR [35] and StringTie [36], with the *A. thaliana*
337 genome (TAIR10) as a reference for mapping.

338 **ChIP-Seq**

339 The fixation of *A. thaliana* T87 cells, chromatin isolation and fragmentation and ChIP (antibody:
340 anti-H3K9me2 (MABI, 308-32361)) were performed basically as described by Saleh *et al.* [37].
341 Successful enrichment of ChIPed DNA was validated according to To *et al.* [38]. ChIP-Seq
342 libraries were prepared using the DNA SMART ChIP-Seq Kit (Takara Clontech), according to
343 the manufacturer's instructions. Libraries were sequenced on an Illumina MiSeq sequencer with
344 76 bp paired-end reads. The sequences derived from a template-switching reaction were
345 trimmed from the reads. Subsequently, the reads from two replicated experiments were
346 combined and mapped to the *A. thaliana* genome (TAIR10) using Bowtie2 [39]. Peaks
347 corresponding to H3K9me2 enrichment were called using MACS (version 2) [40].

348

349 Acknowledgments

350 We thank A. Katahata, I. Ohshima and M. Mino for useful discussions. *Arabidopsis* T87
351 suspension-cultured cells (rpc00008) were provided by RIKEN BRC which is participating in the
352 National Bio-Resource Project of the MEXT, Japan.

353

354 Refereneces

355 1. Soucy SM, Huang J, Gogarten JP. Horizontal gene transfer: building the web of life. Nat Rev
356 Genet. 2015;16(8):472–482. doi: 10.1038/nrg3962.
357 2. Husnik F, McCutcheon JP. Functional horizontal gene transfer from bacteria to eukaryotes.
358 Nat Rev Microbiol. 2018;16(2):67–79. doi: 10.1038/nrmicro.2017.137.

359 3. Timmis JN, Ayliffe MA, Huang CY, Martin W. Endosymbiotic gene transfer: organelle
360 genomes forge eukaryotic chromosomes. Nat Rev Genet. 2004;5(2):123–135. doi:
361 10.1038/nrg1271.
362 4. Matsuo M, Ito Y, Yamauchi R, Obokata J. The rice nuclear genome continuously integrates,
363 shuffles, and eliminates the chloroplast genome to cause chloroplast-nuclear DNA flux. Plant
364 Cell. 2005;17(3):665–675. doi: 10.1105/tpc.104.027706.
365 5. Bock R. Witnessing Genome Evolution: Experimental Reconstruction of Endosymbiotic and
366 Horizontal Gene Transfer. Annu Rev Genet. 2017;51:1–22. doi: 10.1146/annurev-genet-
367 120215-035329.
368 6. Kadowaki K, Kubo N, Ozawa K, Hirai A. Targeting presequence acquisition after
369 mitochondrial gene transfer to the nucleus occurs by duplication of existing targeting signals.
370 EMBO J. 1996;15(23):6652–6661. doi: 10.1002/j.1460-2075.1996.tb01055.x
371 7. Kubo N, Harada K, Hirai A, Kadowaki K. A single nuclear transcript encoding mitochondrial
372 RPS14 and SDHB of rice is processed by alternative splicing: common use of the same
373 mitochondrial targeting signal for different proteins. Proc Natl Acad Sci U S A.
374 1999;96(16):9207–9211. doi: 10.1073/pnas.96.16.9207.
375 8. Fobert PR, Labbé H, Cosmopoulos J, Gottlob-McHugh S, Ouellet T, Hattori J, et al. T-DNA
376 tagging of a seed coat-specific cryptic promoter in tobacco. Plant J. 1994;6(4):567–577. doi:
377 10.1046/j.1365-313x.1994.6040567.x.
378 9. Topping JF, Agyeman F, Henricot B, Lindsey K. Identification of molecular markers of
379 embryogenesis in Arabidopsis thaliana by promoter trapping. Plant J. 1994;5(6):895–903. doi:
380 10.1046/j.1365-313x.1994.5060895.x.
381 10. Mollier P, Hoffmann B, Orsel M, Pelletier G. Tagging of a cryptic promoter that confers root-
382 specific gus expression in Arabidopsis thaliana. Plant Cell Rep. 2000;19(11):1076–1083. doi:
383 10.1007/s002990000241.
384 11. Plesch G, Kamann E, Mueller-Roeber B. Cloning of regulatory sequences mediating guard-
385 cell-specific gene expression. Gene. 2000;249(1-2):83–89. doi: 10.1016/s0378-1119(00)00150-
386 5.

387 12. Yamamoto YY, Tsuhara Y, Gohda K, Suzuki K, Matsui M. Gene trapping of the Arabidopsis
388 genome with a firefly luciferase reporter. Plant J. 2003;35(2):273–283. doi: 10.1046/j.1365-
389 313x.2003.01797.x.
390 13. Sivanandan C, Sujatha TP, Prasad AM, Resminath R, Thakare DR, Bhat SR, et al. T-DNA
391 tagging and characterization of a cryptic root-specific promoter in Arabidopsis. Biochim Biophys
392 Acta. 2005;1731(3):202–208. doi: 10.1016/j.bbaexp.2005.10.006.
393 14. Stangeland B, Nestestog R, Grini PE, Skrbo N, Berg A, Salehian Z, et al. Molecular analysis
394 of Arabidopsis endosperm and embryo promoter trap lines: reporter-gene expression can result
395 from T-DNA insertions in antisense orientation, in introns and in intergenic regions, in addition
396 to sense insertion at the 5' end of genes. J Exp Bot. 2005;56(419):2495–2505. doi:
397 10.1093/jxb/eri242.
398 15. Kudo H, Matsuo M, Satoh S, Hachisu R, Nakamura M, Yamamoto Y, Yoshiharu, et al.
399 Cryptic promoter activation occurs by at least two different mechanisms in the *Arabidopsis*
400 genome. BioRxiv [Preprint]. bioRxiv [posted 2020 Nov 28]. Available from:
401 https://www.biorxiv.org/content/10.1101/2020.11.28.399337v1 doi: 10.1101/2020.11.28.399337
402 16. Akhtar W, de Jong J, Pindyurin AV, Pagie L, Meuleman W, de Ridder J, et al. Chromatin
403 position effects assayed by thousands of reporters integrated in parallel. Cell. 2013;154(4):914–
404 927. doi: 10.1016/j.cell.2013.07.018.
405 17. Inoue F, Ahituv N. Decoding enhancers using massively parallel reporter assays. Genomics.
406 2015;106(3):159–164. doi: 10.1016/j.ygeno.2015.06.005.
407 18. Shu H, Wildhaber T, Siretskiy A, Gruissem W, Hennig L. Distinct modes of DNA
408 accessibility in plant chromatin. Nat Commun. 2012;3:1281. doi: 10.1038/ncomms2259.
409 19. Bühler M, Moazed D. Transcription and RNAi in heterochromatic gene silencing. Nat Struct
410 Mol Biol. 2007;14(11):1041–1048. doi: 10.1038/nsmb1315.
411 20. Grewal SI, Jia S. Heterochromatin revisited. Nat Rev Genet. 2007;8(1):35–46. doi:
412 10.1038/nrg2008.
413 21. Bernatavichute YV, Zhang X, Cokus S, Pellegrini M, Jacobsen SE. Genome-wide
414 association of histone H3 lysine nine methylation with CHG DNA methylation in Arabidopsis
415 thaliana. PLoS One. 2008;3(9):e3156. doi: 10.1371/journal.pone.0003156.

416 22. Magori S, Citovsky V. Epigenetic control of Agrobacterium T-DNA integration. Biochim
417 Biophys Acta. 2011;1809(8):388–394. doi: 10.1016/j.bbagrm.2011.01.007.
418 23. Kleinboelting N, Huep G, Appelhagen I, Viehoever P, Li Y, Weisshaar B. The Structural
419 Features of Thousands of T-DNA Insertion Sites Are Consistent with a Double-Strand Break
420 Repair-Based Insertion Mechanism. Mol Plant. 2015;8(11):1651–1664. doi:
421 10.1016/j.molp.2015.08.011.
422 24. Soria G, Polo SE, Almouzni G. Prime, repair, restore: the active role of chromatin in the
423 DNA damage response. Mol Cell. 2012;46(6):722–734. doi: 10.1016/j.molcel.2012.06.002.
424 25. Dabin J, Fortuny A, Polo SE. Epigenome Maintenance in Response to DNA Damage. Mol
425 Cell. 2016;62(5):712–727. doi: 10.1016/j.molcel.2016.04.006.
426 26. Wang Y, Wang A, Liu Z, Thurman AL, Powers LS, Zou M, et al. Single-molecule long-read
427 sequencing reveals the chromatin basis of gene expression. Genome Res. 2019;29(8):1329–
428 1342. doi: 10.1101/gr.251116.119.
429 27. Shipony Z, Marinov GK, Swaffer MP, Sinnott-Armstrong NA, Skotheim JM, Kundaje A, et al.
430 Long-range single-molecule mapping of chromatin accessibility in eukaryotes. Nat Methods.
431 2020;17(3):319–327. doi: 10.1038/s41592-019-0730-2.
432 28. Stergachis AB, Debo BM, Haugen E, Churchman LS, Stamatoyannopoulos JA. Single-
433 molecule regulatory architectures captured by chromatin fiber sequencing. Science.
434 2020;368(6498):1449–1454. doi: 10.1126/science.aaz1646.
435 29. Hellens RP, Edwards EA, Leyland NR, Bean S, Mullineaux PM. pGreen: a versatile and
436 flexible binary Ti vector for Agrobacterium-mediated plant transformation. Plant Mol Biol.
437 2000;42(6):819–832. doi: 10.1023/A:1006496308160
438 30. Hirashima M, Satoh S, Tanaka R, Tanaka A. Pigment shuffling in antenna systems
439 achieved by expressing prokaryotic chlorophyllide a oxygenase in Arabidopsis. J Biol Chem.
440 2006;281(22):15385–15393. doi: 10.1074/jbc.M602903200.
441 31. Axelos M, Curie C, Mazzolini L, Bardet C, Lescure B. A protocol for transient gene
442 expression in Arabidopsis thaliana protoplasts isolated from cell suspension cultures. Plant
443 Physiol Biochem. 1992;30:123–128.
444 32. Ogawa Y, Dansako T, Yano K, Sakurai N, Suzuki H, Aoki K, et al. Efficient and high-
445 throughput vector construction and Agrobacterium-mediated transformation of Arabidopsis

446 thaliana suspension-cultured cells for functional genomics. Plant Cell Physiol. 2008;49(2):242–
447 250. doi: 10.1093/pcp/pcm181.
448 33. Hata T, Mukae K, Satoh S, Matsuo M, Obokata J. Preculture in an enriched nutrient
449 medium greatly enhances the *Agrobacterium*-mediated transformation efficiency in *Arabidopsis*
450 T87 cultured cells. Plant Biotechnology. 2020. doi: 10.5511/plantbiotechnology.20.12.11b.
451 34. Langmead B, Trapnell C, Pop M, Salzberg SL. Ultrafast and memory-efficient alignment of
452 short DNA sequences to the human genome. Genome Biol. 2009;10(3):R25. doi: 10.1186/gb-
453 2009-10-3-r25.
454 35. Dobin A, Davis CA, Schlesinger F, Drenkow J, Zaleski C, Jha S, et al. STAR: ultrafast
455 universal RNA-seq aligner. Bioinformatics. 2013;29(1):15–21. doi:
456 10.1093/bioinformatics/bts635.
457 36. Pertea M, Pertea GM, Antonescu CM, Chang TC, Mendell JT, Salzberg SL. StringTie
458 enables improved reconstruction of a transcriptome from RNA-seq reads. Nat Biotechnol.
459 2015;33(3):290–295. doi: 10.1038/nbt.3122.
460 37. Saleh A, Alvarez-Venegas R, Avramova Z. An efficient chromatin immunoprecipitation
461 (ChIP) protocol for studying histone modifications in Arabidopsis plants. Nat Protoc.
462 2008;3(6):1018–1025. doi: 10.1038/nprot.2008.66.
463 38. To TK, Kim JM, Matsui A, Kurihara Y, Morosawa T, Ishida J, et al. Arabidopsis HDA6
464 regulates locus-directed heterochromatin silencing in cooperation with MET1. PLoS Genet.
465 2011;7(4):e1002055. doi: 10.1371/journal.pgen.1002055.
466 39. Langmead B, Salzberg SL. Fast gapped-read alignment with Bowtie 2. Nat Methods.
467 2012;9(4):357–359. doi: 10.1038/nmeth.1923.
468 40. Zhang Y, Liu T, Meyer CA, Eeckhoute J, Johnson DS, Bernstein BE, et al. Model-based
469 analysis of ChIP-Seq (MACS). Genome Biol. 2008;9(9):R137. doi: 10.1186/gb-2008-9-9-r137.

470

471 # Figure legends

472 **Fig 1. Massively parallel promoter-trapping analysis of the *Arabidopsis thaliana* genome.**
473 (A) Genomic positions of the inserted promoterless *LUC* genes and respective transcription
474 levels. The bars represent the 4,504 mapped *LUC* genes regarding their orientation towards the

475 upper (+) or bottom (–) DNA strands of the five *A. thaliana* chromosomes. The colour scheme
476 discriminates *LUC* genes according to their expression levels. (B) Relative abundance of the
477 *LUC* gene insertion types relative to the annotated gene locations. The *LUC* genes that cannot
478 be classified their insertion type uniquely were omitted. (C) Percentage of transcribed *LUC*
479 genes within the respective insertion types. S and AS indicate the sense and antisense
480 orientations, respectively. (D) Distribution profiles of the *LUC* genes of respective insertion
481 types according to the transcription level, with the total frequency of each insertion type
482 normalized to be 100%. The light-blue area indicates the superposed fraction in the genic-
483 sense insertion type. (E) Abundance of the *LUC* genes with the indicated transcription levels in
484 relation to the distance from the genic TSS in each window (200 bp). (F) Classification of the
485 transcribed *LUC* genes according to their insertion types, as in (B).

486 **Fig 2. Transcription states of the *LUC* loci in WT and transgenic cells.** (A) The 4,504 *LUC*
487 loci were clustered into four groups according to the combination of on/off transcription states in
488 WT and transgenic cells. The local transcription landscape in WT cells was determined based
489 on the RNA-Seq analysis. (B) Comparison of the transcription levels between WT and
490 transgenic cells for the *LUC* loci that were transcribed in both WT and transgenic cells.

491 **Fig 3. Transcription states of the *LUC* genes in the heterochromatic regions.** (A) The
492 upper panel shows the transcription profile of the *LUC* genes in the heterochromatic regions.
493 The middle and bottom panels are derived from Fig 1D and represent the transcription profiles
494 of the genic-sense type and all of the *LUC* genes, respectively. H3K9me2-marked
495 heterochromatic regions covered 18.6 Mb in total and accounted for ~15.6% of the genome,
496 where 120 *LUC* genes were inserted. About 80% of the H3K9me2-marked regions lay within
497 the pericentromere. (B) Transcription levels of the *LUC* genes relative to the increased
498 enrichment of H3K9me2. The transcription levels and H3K9me2 enrichment are both shown as
499 percentiles based on all of the *LUC* genes located in the H3K9me2-marked heterochromatic
500 regions.

501 **Fig 4. Transcriptional states of neighbouring *LUC* insert pairs located in close proximity.**
502 (A) *LUC* pairs inserted in close proximal chromosomal regions were used for integration-
503 neighbourhood analysis. (B) Three possible fates of the transcription of *LUC* pairs: Fate A,

504 expression of both *LUC* genes; Fate B, expression of one *LUC* gene and silencing of the other;
505 and Fate C: silencing of both *LUC* genes. (C and D) Expected ratio of the three transcriptional
506 fates classified in (B) for *LUC* pairs obeying (C) locus-dependent activation or (D) integration-
507 dependent stochastic activation. (E) Transcriptional states of neighbouring *LUC* pairs inserted
508 in the different cells. The distances between each neighbouring *LUC* insert were <50 bp (upper
509 panel, n = 21) and <10 bp (lower panel, n = 12). (F) Measured and expected number of *LUC*
510 pairs with Fate A, Fate B, and Fate C, as described in (E). The expected number was
511 calculated according to the integration-dependent stochastic activation, assuming each
512 transcriptional activation rate as 30%.

513

514 Supporting information captions

515 **S1 Fig. Precise workflow of the promoter analysis that was performed using the TRIP**
516 **system.** (A) Transformation of multiplexed barcoded vectors into *Arabidopsis* T87 suspension-
517 cultured cells. (B) Preparation of sequencing libraries for the mapping and expression analyses.
518 To prepare the mapping libraries, two different methods were employed after inverse PCR. In
519 the first method, nested PCR products were fragmented and tagged with sequencing adapters
520 using a Nextera-based method. In another method, inverse PCR products were subjected to
521 tailed PCR, to add the sequencing adapters. To prepare libraries for the expression analysis,
522 the barcode regions of both cellular DNA and cDNA were PCR amplified, followed by the
523 addition of sequencing adapters using tailed PCR. cDNAs were prepared via an oligo(dT)-
524 primed RT reaction. The libraries obtained were applied to a high-throughput sequencing
525 analysis. (C) Workflow of the data-analysis pipeline that was used for the mapping of *LUC*
526 genes. The flanking sequences of the *LUC* genes were extracted from the Nextera-based
527 mapping library and tailed-PCR-based mapping library using slightly different methods. The
528 *LUC* loci obtained were combined in the final step. (D) Flow diagram used for the
529 determination of *LUC* transcription levels. The transcription level data obtained for
530 individual barcodes were associated with the respective mapped *LUC* genes and used
531 in subsequent analyses.

532 **S2 Fig. Validation of the *LUC* mapped loci and barcode sequences via PCR amplification**
533 **in five representative samples.** (A) Schematic diagram of the nested PCR that was performed
534 using insertion-site-specific and *LUC*-specific primers. (B) Five *LUC* genes were chosen from
535 the TRIP-Pool1 and detected by PCR. PC1 and PC2 are technical replicates of the PCR using
536 the template DNA from TRIP-Pool1 cells. NC is the PCR product from the DNA of TRIP-Pool2
537 and was used as a negative control. The PCR products were loaded onto a 2% agarose gel.
538 The expected size of the PCR products is shown at the top of the gel, in parentheses. The PCR
539 products obtained were Sanger sequenced for verification of the barcode sequences.

540 **S3 Fig. Length of each genomic context.** The total length of the respective genomic contexts
541 and their percentage in the whole genome are shown. The 200 bp segments 5′-proximal to the
542 genic region (CDS plus UTR regions according to TAIR10) were defined as promoter regions,
543 and the remaining sequences were defined as intergenic regions. When neighboring promoter
544 and genic regions were overlapped, those parts were omitted from the statistical analyses
545 described above (their sum was 0.23 Mb, 0.2% of the whole genome).

546 **S4 Fig. Abundances of *LUC* genes relative to the nearest genic TSS.** Number of LUC
547 genes in relation to the distances from the genic TSS was counted in 200 bp window size.

548 **S5 Fig. Assessment of the effect of barcode sequences on the LUC transcription levels.**
549 Frequently observed barcode motifs in the LUC insert of indicated transcription levels were
550 analyzed using WebLogo3 (Crooks *et al.*, 2004). The transcription levels of all the LUC genes
551 are shown as in Fig 1D. A weak positional preference for ‘A’ was found at the 3′-terminal
552 position on the barcode. However, the frequency of ‘A’ at this position did not correlate with the
553 strength of transcription.

554 **S6 Fig. Similarity/dissimilarity of the transcription levels of the randomly selected LUC**
555 **pairs against the sequence identity of the 12-base barcode.** A pair of LUC genes was
556 randomly selected from the 4,504 mapped LUC genes, and the similarity/dissimilarity of their
557 transcription levels is shown as the ratio of their RNA levels in a logarithmic scale; the ratio was
558 calculated by dividing the higher RNA level by the lower level (i.e., log(ratio) ≥0). The
559 similarity/diversity of the barcode is indicated by the number of mismatched nucleotides at the
560 corresponding positions. This graph is the summary of the analysis of 10,566 LUC pairs and

561 indicates the absence of a correlation between the similarity of the barcode sequence and that
562 of the transcription level. In other words, the barcode sequence does not affect the transcription
563 level of LUC genes.

564 Methods note: 1) When randomly selected LUC pairs were located within 100 kb on the
565 same chromosome, they were omitted from the analysis, lest their positional effect should
566 influence their transcription levels. 2) One thousand LUC pairs were analyzed each for the
567 indicated number of mismatches in the barcode. However, for mismatch numbers of 0, 1, and 2,
568 the number of LUC pairs analyzed was 92, 51, and 423, respectively. This is because the
569 number of such highly homologous barcodes in the total population of 4,504 LUC inserts was
570 limited, and these are all the LUC genes that fulfilled the given requests. 3) The LUC inserts of
571 the identical barcodes were derived from different TRIP pools, because LUC mapping in a
572 given TRIP pool had been conducted so that the individual LUC genes were mapped to a
573 unique locus, with omission of those that were mapped to more than one locus.

574 **S7 Fig. Frequency of transcribed *LUC* genes relative to the annotated genic TSS.**
575 Abundance of the *LUC* genes with the indicated transcription levels in relation to the distance
576 from the genic TSS, as shown in Fig 1E. The plot was smoothed by calculating the five-point
577 moving average of integration frequency in each window (200 bp).

578 **S8 Fig. Expression profiles of *LUC* genes with high-number reads from the amplicon-**
579 **sequencing data and of *LUC* genes from biological replicates.** (A and B) For each barcode,
580 when the number of reads from DNA amplicon sequencing was up to (A) 100 or (B) 1,000, the
581 barcode was omitted from the analysis. The number of reads for each barcode obtained from
582 RNA amplicon sequencing was redefined as zero, if the number of reads was below such
583 thresholds. The subsequent processes used in this analysis were same as those used in Fig 1D.
584 The expression profiles of the *LUC* genes located in promoter regions were omitted from (B),
585 because the number of such *LUC* genes was insufficient to represent their profiles. (C–E)
586 Expression profiles of three biological replicates. The numbers of *LUC* genes shown in all
587 graphs are the total amount of *LUC* genes used for their analysis. The fraction of the
588 transcribed *LUC* genes attributed by two distinct mechanisms are indicated by light-blue and
589 light-red areas.

590 **S9 Fig. Two examples of transcribed LUC genes in the H3K9me2-marked regions located**
591 **around the centromere.** (A and B) Transcribed LUC genes (asterisk) were found 63 kb and
592 682 kb away from the centromeres of chromosomes 2 (A) and 5 (B), respectively. The
593 respective H3K9me2 levels of these loci were 80 (A) and 91 (B) percentiles, respectively. In WT
594 T87 cells, transcripts were very scarce in these heterochromatic regions.

595 **S10 Fig. Distribution of *cis*-regulatory elements in the upstream region of *LUC***
596 **integration sites.** (A and B) The frequency of TATA-box, Y patch, and GA elements in the
597 upstream region of the (A) TSS of annotated genes, or (B) of ATG initiation codons of
598 annotated genes and 5′ ends of *LUC* inserts were analyzed according to Yamamoto *et al.*
599 (Yamamoto *et al.*, 2007) using a window size of 50 bp for the high-sensitive detection of the
600 motifs. The Y-axis represents the fraction of genes or *LUC* genes that contained the indicated
601 motifs.

602 **S1 Table. Primer list**

603 **S1 Methods. Detailed methods for the massive promoter-trapping experiment**

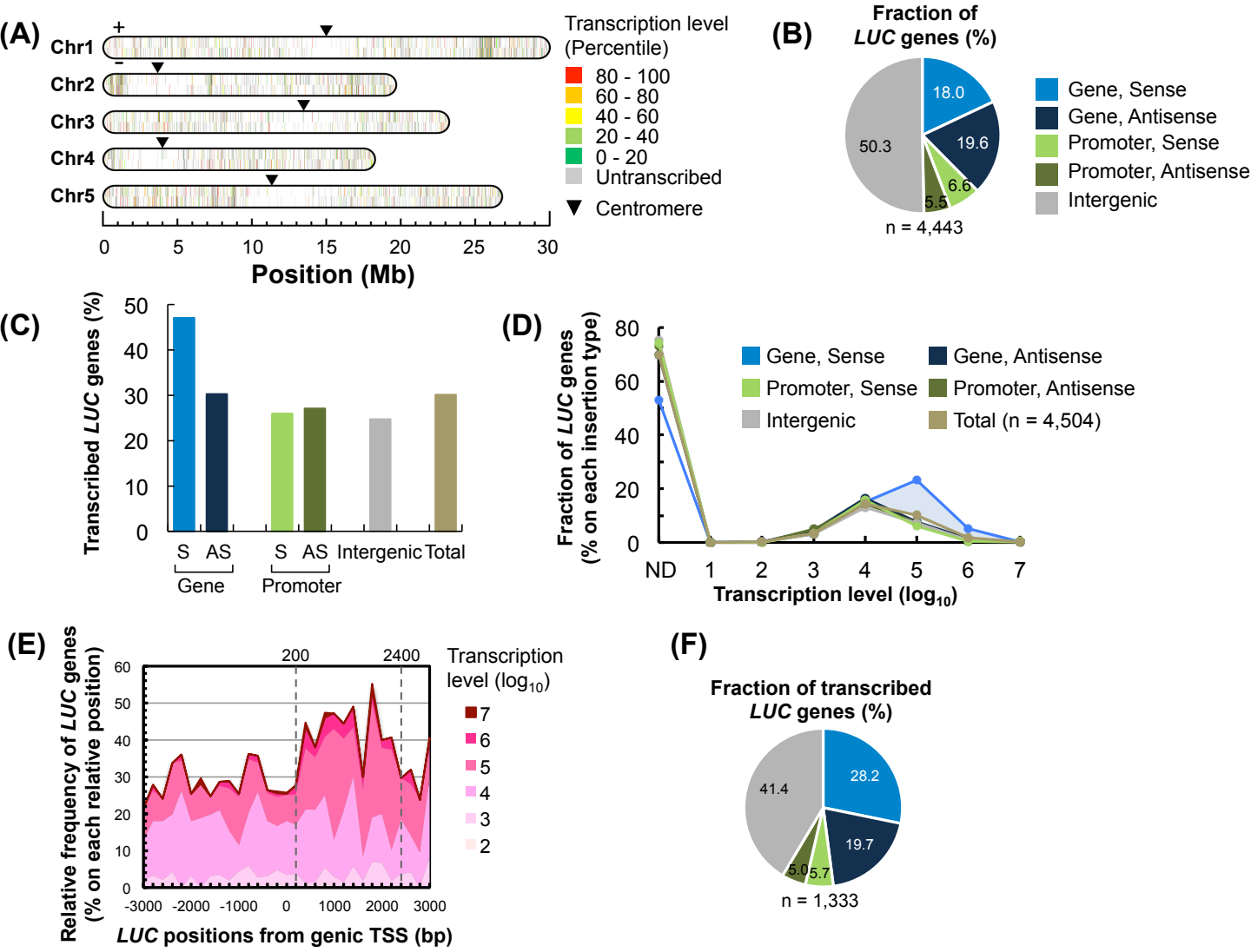

Fig 1. Massively parallel promoter-trapping analysis of the *Arabidopsis thaliana* genome. (A) Genomic positions of the inserted promoterless *LUC* genes and respective transcription levels. The bars represent the 4,504 mapped *LUC* genes regarding their orientation towards the upper (+) or bottom (–) DNA strands of the five *A. thaliana* chromosomes. The colour scheme discriminates *LUC* genes according to their expression levels. (B) Relative abundance of the *LUC* gene insertion types relative to the annotated gene locations. The *LUC* genes that cannot be classified their insertion type uniquely were omitted. (C) Percentage of transcribed *LUC* genes within the respective insertion types. S and AS indicate the sense and antisense orientations, respectively. (D) Distribution profiles of the *LUC* genes of respective insertion types according to the transcription level, with the total frequency of each insertion type normalized to be 100%. The light-blue area indicates the superposed fraction in the genic-sense insertion type. (E) Abundance of the *LUC* genes with the indicated transcription levels in relation to the distance from the genic TSS in each window (200 bp). (F) Classification of the transcribed *LUC* genes according to their insertion types, as in (B).

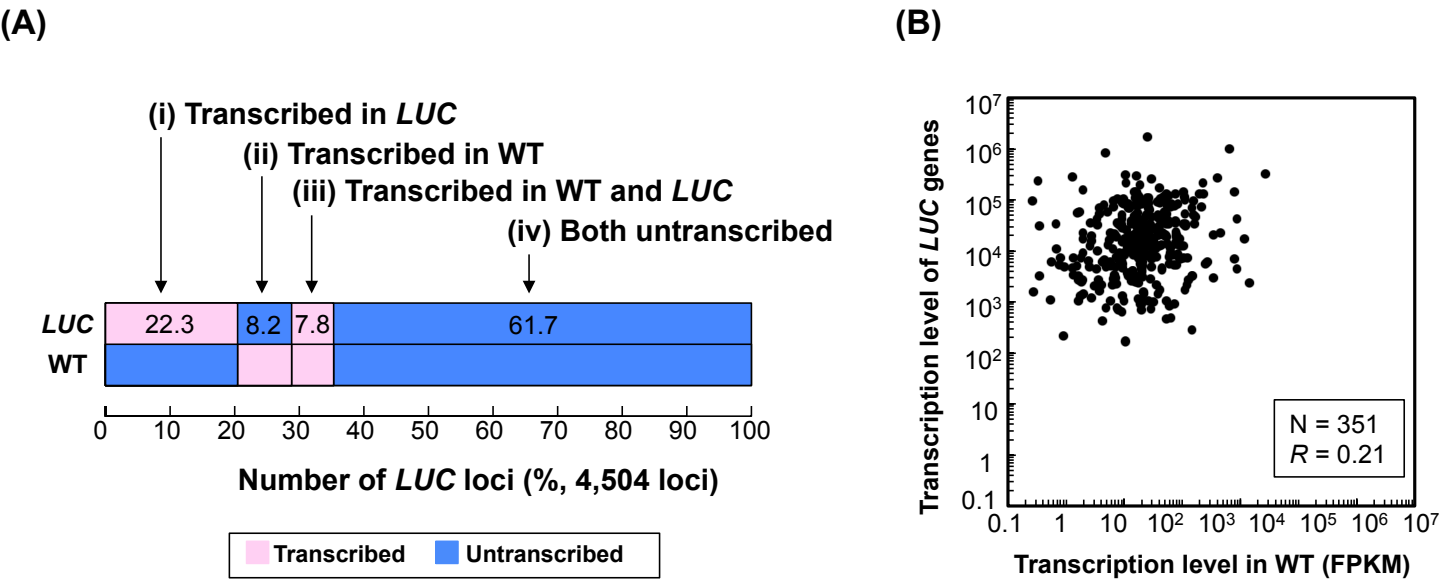

Fig 2. Transcription states of the *LUC* loci in WT and transgenic cells. (A) The 4,504 *LUC* loci were clustered into four groups according to the combination of on/off transcription states in WT and transgenic cells. The local transcription landscape in WT cells was determined based on the RNA-Seq analysis. (B) Comparison of the transcription levels between WT and transgenic cells for the *LUC* loci that were transcribed in both WT and transgenic cells.

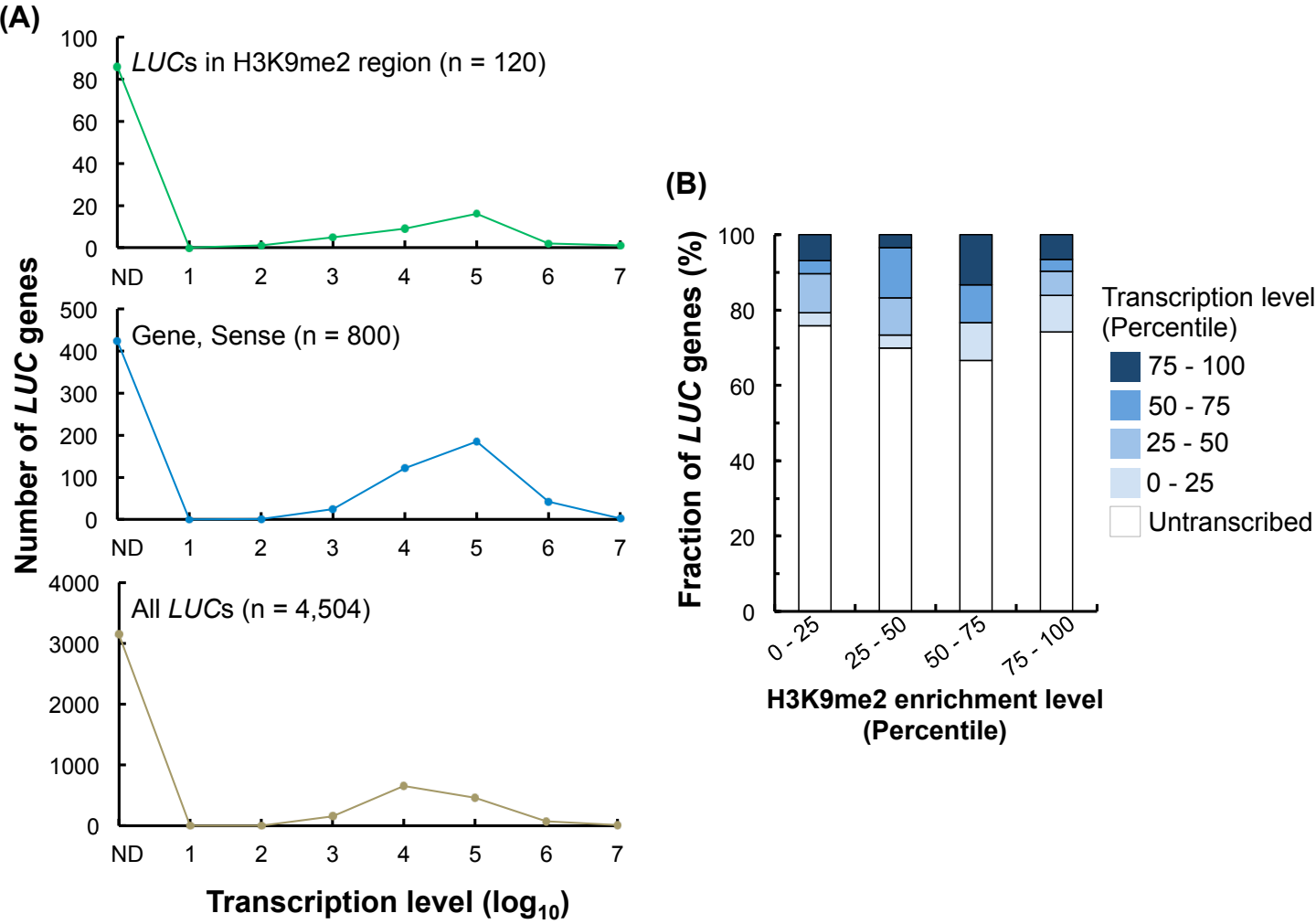

Fig 3. Transcription states of the *LUC* genes in the heterochromatic regions. (A) The upper panel shows the transcription profile of the *LUC* genes in the heterochromatic regions. The middle and bottom panels are derived from Fig 1D and represent the transcription profiles of the genic-sense type and all of the *LUC* genes, respectively. H3K9me2-marked heterochromatic regions covered 18.6 Mb in total and accounted for ~15.6% of the genome, where 120 *LUC* genes were inserted. About 80% of the H3K9me2-marked regions lay within the pericentromere. (B) Transcription levels of the *LUC* genes relative to the increased enrichment of H3K9me2. The transcription levels and H3K9me2 enrichment are both shown as percentiles based on all of the *LUC* genes located in the H3K9me2-marked heterochromatic regions.

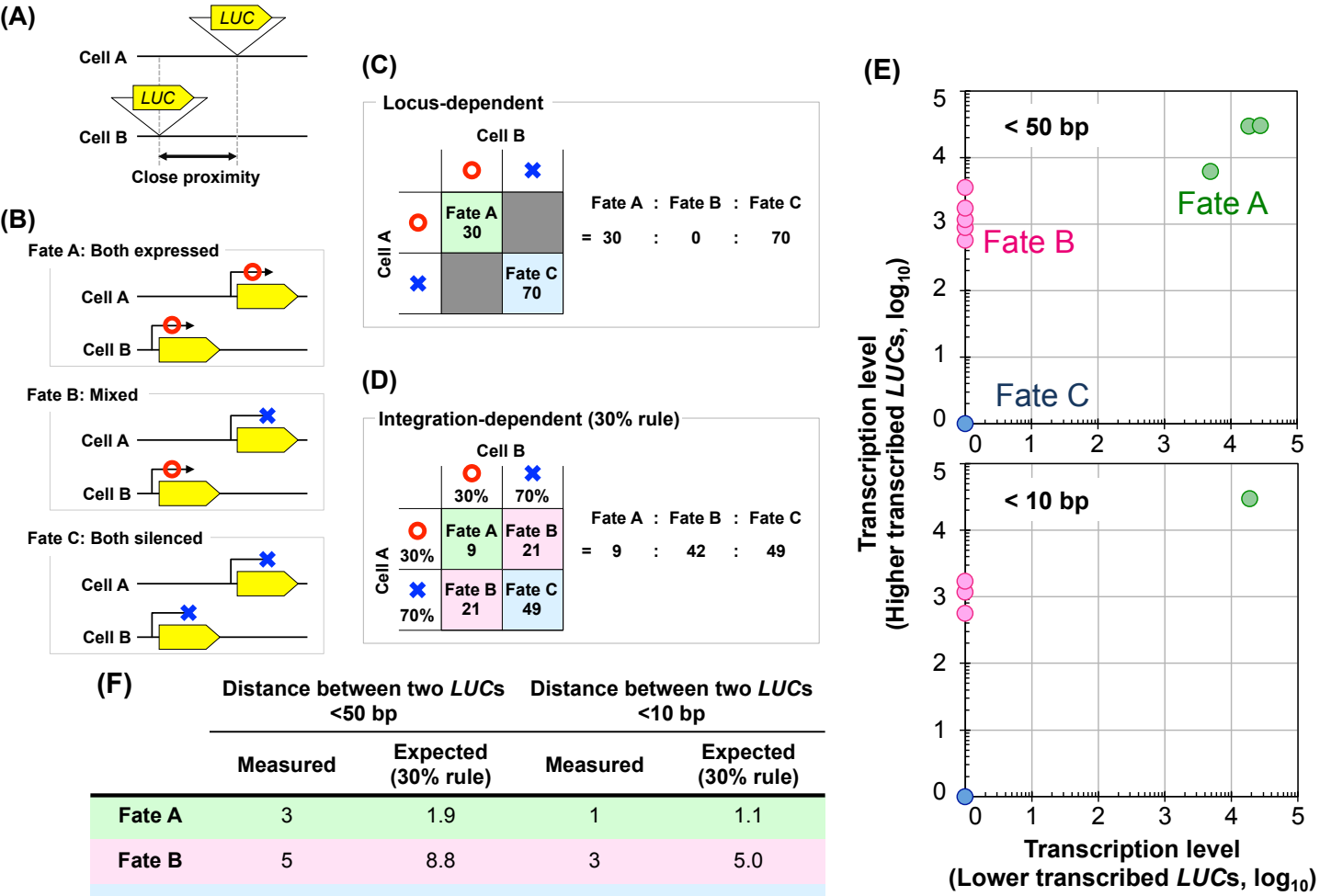

(F)

	Distance between two *LUC*s <50 bp		Distance between two *LUC*s <10 bp	
	Measured	Expected (30% rule)	Measured	Expected (30% rule)
Fate A	3	1.9	1	1.1
Fate B	5	8.8	3	5.0
Fate C	13	10.2	8	5.9
Total	21	21	12	12
Fischer's exact test	$P = 0.55$		$P = 0.82$	

Fig 4. Transcriptional states of neighbouring *LUC* insert pairs located in close proximity. (A) *LUC* pairs inserted in close proximal chromosomal regions were used for integration-neighbourhood analysis. (B) Three possible fates of the transcription of *LUC* pairs: Fate A, expression of both *LUC* genes; Fate B, expression of one *LUC* gene and silencing of the other; and Fate C: silencing of both *LUC* genes. (C and D) Expected ratio of the three transcriptional fates classified in (B) for *LUC* pairs obeying (C) locus-dependent activation or (D) integration-dependent stochastic activation. (E) Transcriptional states of neighbouring *LUC* pairs inserted in the different cells. The distances between each neighbouring *LUC* insert were <50 bp (upper panel, n = 21) and less than 10 bp (lower panel, n = 12). (F) Measured and expected number of *LUC* pairs with Fate A, Fate B, and Fate C, as described in (E). The expected number was calculated according to the integration-dependent activation mechanism.

S1 Methods

Construction of barcoded plasmid libraries.

The transformation vector plasmid was constructed using a modified pGreenII vector [1, 2] to encode a promoter-less reporter cassette and a kanamycin-resistant cassette between the right (RB) and left border (LB) (S1A Fig). The reporter cassette consisted of a 12-base random barcode sequence, the firefly luciferase (*LUC*$^{+}$) gene, and a *nos* terminator sequence, and contained the short sequence 5′–AGGCCTCGAGGTTATCAGCTTACAG–3′ (the *Xho*I site is underlined) between the RB and the random barcode. This short sequence was inserted for the sake of introducing the barcode sequence and also for the construction of amplicon-sequencing libraries. The kanamycin-resistant cassette contained the *NptII* gene with a *nos* promoter and *nos* terminator. The LB was modified to be repeated four times (S1A Fig), to suppress the integration of the vector backbone sequence into the plant genome [3]. The modified LB sequence was 5′–ATCCTGCCAGTTACACCACAATATATCCTGCCAGTTACACCACAATATATCCTGCCAGTTACACCACAATATATCCTGCCAGTTACACCACAATATATCCTGCCA–3′, and the first 9 bases were added through the construction step. To obtain a plasmid library that contained the random barcode sequence, the 5′-end fragment of the luciferase gene was amplified using two primers (5′–AAAGTCGACGTTATCAGCTTACAGNNNNNNNNNNNNATGGAAGACGCCAAAAACAT–3′ and 5′–TTAGGTAACCCAGTAGATCCAGAGG–3′ (the *Sal*I site is underlined)), digested with *Sal*I and *Eco*RI (the *Eco*RI site was located on the amplified *LUC* fragment), and inserted into the *Xho*I and *Eco*RI sites of the transformation vector.

The constructed vector was transformed into *Escherichia coli* strain NEB 10-beta (New

England Bilabs) by electroporation, and approximately 420,000 transformant colonies were obtained; this number suggests the initial diversity of the barcode clones. The transformed *E. coli* cells were cultured in liquid LB medium and subjected to plasmid DNA extraction.

Mapping of the *LUC* genomic loci.

The high-throughput sequencing data of the mapping libraries were trimmed from the 3′ end using fastq_quality_trimmer (http://hannonlab.cshl.edu/fastx_toolkit/) with a phred-scaled quality score ≥30 and were used for the mapping of *LUC* genes with the aid of open-source software and custom Perl scripts (S1C Fig). In *Agrobacterium*-mediated DNA integration, the 3′-terminal 3 bp of the RB is usually the junction between the T-DNA and the plant genome [4]. Therefore, the transformation vector sequence from the 3′-terminal 3 bp of the RB to the ATG initiation codon of *LUC* was used as the *LUC* segment, to search for the *LUC* flanking genomic sequences. The searching methods were slightly different between the two types of mapping libraries. (i) In the Nextera-based libraries, both paired-end reads were used to obtain *LUC* flanking sequences. Sequenced reads that included the *LUC* segment plus more than 25 bp of its flanking sequence were screened, and the flanking sequences and their corresponding *LUC* barcodes were extracted. The flanking sequences obtained were trimmed up to 50 bp using fastx_trimmer (http://hannonlab.cshl.edu/fastx_toolkit/). (ii) In the tailed-PCR libraries, only forward reads from the paired-end reads were used for the extraction of *LUC* flanking sequences, and their 3′-terminal 157 bp segments were removed using fastx_trimmer. From the obtained reads, 25-bp flanking sequences of the *LUC* segments and their corresponding barcodes were extracted as described above.

The flanking sequences obtained above were mapped to the *Arabidopsis* genome of TAIR10 version using Bowtie [5], on the condition that, at most, three mismatches were allowed and that individual sequences were associated with a unique genomic locus (Bowtie settings, -m 1, -v 3). Subsequently, the 3′-junction sites of the mapped flanking sequences were defined as the genomic loci of the corresponding *LUC* insertion sites. We also applied the following rules: 1) *LUC* genes that mapped at a single locus but for which the sequence reads were less than 3 were discarded and 2) cases in which very similar barcodes were mapped to identical loci (data not shown) suggested that an error occurred in the high-throughput sequencing of the barcode. Therefore, barcodes that occupied more than 90% of the reads at their respective genomic loci were retained, and their *LUC* genes were mapped to the respective loci.

Finally, we combined all *LUC* loci that were derived from three biologically independent TRIP pools, as well as from two kinds of mapping libraries, and subjected them to the following analyses.

Determination of the transcription levels of *LUC* genes.

Bioinformatics analyses of the *LUC* expression data were performed using a custom Perl script, the Microsoft Excel software, and the R package (http://www.R-project.org).

To compare the expression levels of individual *LUC* genes, their relative transcript levels were determined as follows (S1B and D Fig). The cDNA and DNA libraries that were specifically prepared for the expression analysis were subjected to amplicon sequencing on an Illumina MiSeq sequencer with 76 bp pair-end reads. The barcode sequences obtained were verified by the corresponding reads of each pair-end. The read numbers of each barcode sequences was

counted in each sequencing library. We should note that, after sequencing on the MiSeq apparatus, *LUC* genes with a DNA read number ≤5 were omitted from the subsequent analysis. Besides, when the cDNA read number was ≤5, the transcript levels of the *LUC* genes were set as zero. Subsequently, the cDNA and DNA read numbers of the individual barcodes were normalized to the total cDNA and DNA read numbers of all barcodes, respectively. Then, the normalized cDNA barcode number was divided by the corresponding normalized DNA barcode number, to give an indicator of the RNA level per DNA molecule. This indicative number was multiplied by 10,000 and was used to indicate the transcription levels of the individual *LUC* genes. Obtained transcription levels of each *LUC* gene were then assigned to individual insertion loci described above according to the barcode sequences. *LUC* loci were omitted from subsequent analysis when transcription levels were not assigned.

References

1. Hellens, R.P., Edwards, E.A., Leyland, N.R., Bean, S. and Mullineaux, P.M. (2000) pGreen: a versatile and flexible binary Ti vector for Agrobacterium-mediated plant transformation. Plant Mol Biol., 42, 819–832.
2. Hirashima, M., Satoh, S., Tanaka, R. and Tanaka, A. (2006) Pigment shuffling in antenna systems achieved by expressing prokaryotic chlorophyllide a oxygenase in Arabidopsis. J Biol Chem., 281, 15385–15393.
3. Kuraya, Y., Ohta, S., Fukuda, M., Hiei, Y., Murai, N., Hamada, K., Ueki, J., Imaseki, H. and Komari, T. (2004) Suppression of transfer of non-T-DNA 'vector backbone' sequences by multiple left border repeats in vectors for transformation of higher plants mediated by *Agrobacterium tumefaciens*. Molecular Breeding., 14, 309–320.
4. Windels, P., De Buck, S. and Depicker, A. (2008) Agrobacterium Tumefaciens-Mediated Transformation: Patterns of T-DNA Integration Into the Host Genome. In: Tzfira T, Citovski V, editors. Agrobacterium: From Biology to Biotechnology: Springer, New York, NY, p. 441–481.

5. Langmead, B., Trapnell, C., Pop, M. and Salzberg, S.L. (2009) Ultrafast and memory-efficient alignment of short DNA sequences to the human genome. Genome Biol., 10, R25.

6. Yamamoto, Y.Y., Ichida, H., Matsui, M., Obokata, J., Sakurai, T., Satou, M., Seki, M., Shinozaki, K. and Abe, T. (2007) Identification of plant promoter constituents by analysis of local distribution of short sequences. *BMC Genomics,* 8, 67.

7. Crooks, G. E., Hon, G., Chandonia, J. M. and Brenner, S. E. (2004) WebLogo: a sequence logo generator. *Genome Res,* 14, 1188–1190.

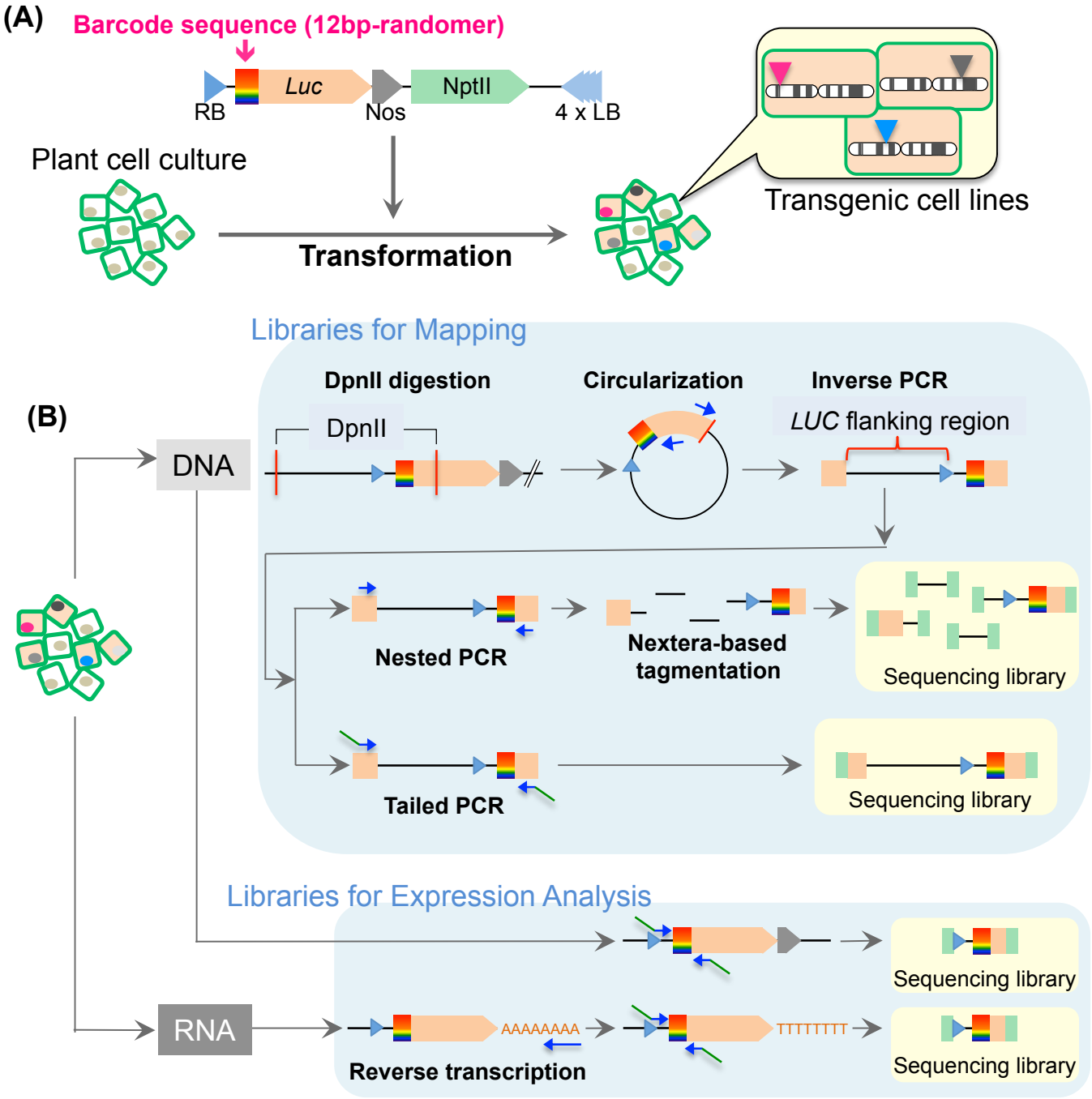

S1 Fig. Precise workflow of the promoter analysis that was performed using the TRIP system. (A) Transformation of multiplexed barcoded vectors into *Arabidopsis* T87 suspension-cultured cells. (B) Preparation of sequencing libraries for the mapping and expression analyses. To prepare the mapping libraries, two different methods were employed after inverse PCR. In the first method, nested PCR products were fragmented and tagged with sequencing adapters using a Nextera-based method. In another method, inverse PCR products were subjected to tailed PCR, to add the sequencing adapters. To prepare libraries for the expression analysis, the barcode regions of both cellular DNA and cDNA were PCR amplified, followed by the addition of sequencing adapters using tailed PCR. cDNAs were prepared via an oligo(dT)-primed RT reaction. The libraries obtained were applied to a high-throughput sequencing analysis.

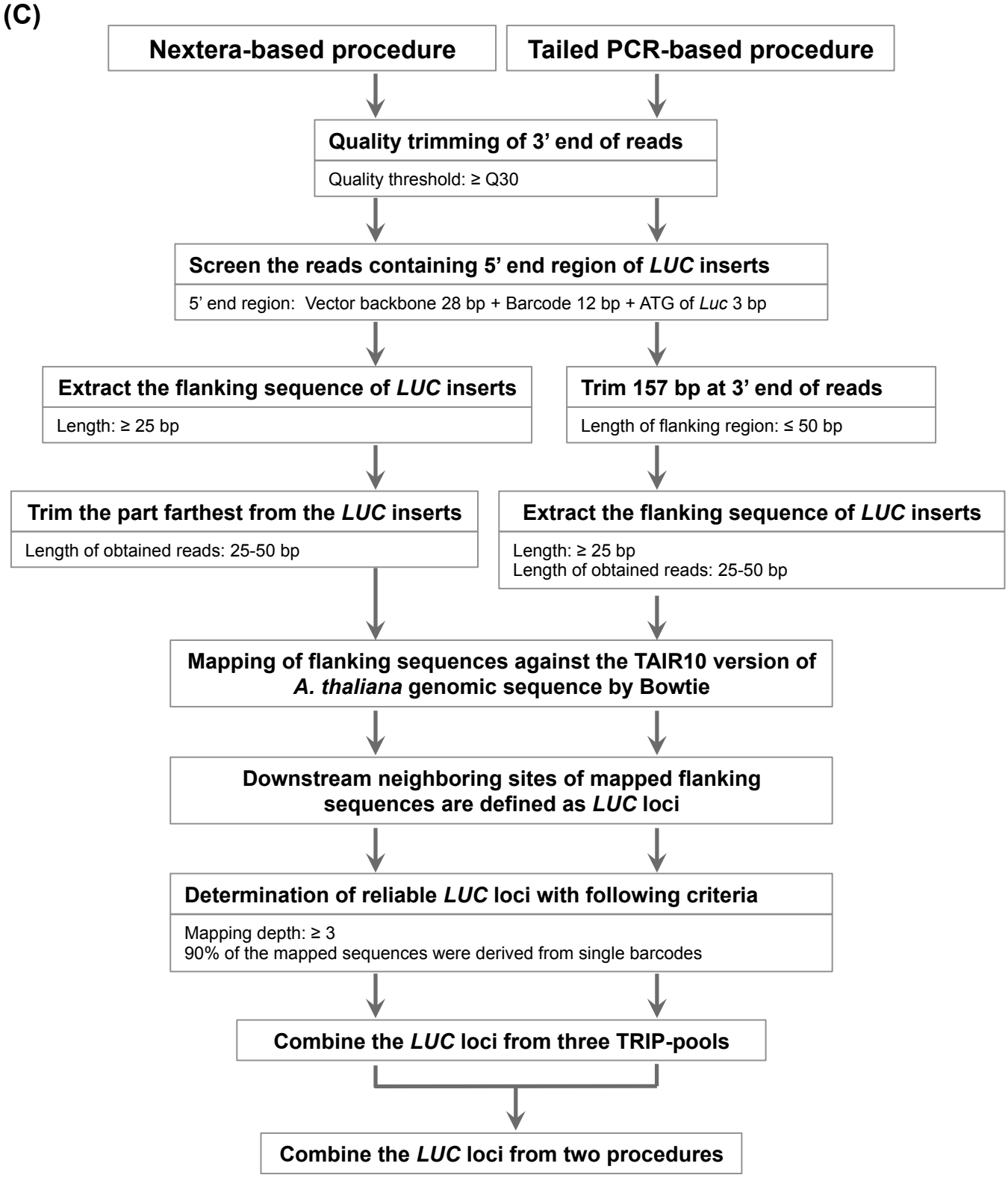

S1 Fig. Precise workflow of the promoter analysis that was performed using the TRIP system. (C) Workflow of the data-analysis pipeline that was used for the mapping of *LUC* genes. The flanking sequences of the *LUC* genes were extracted from the Nextera-based mapping library and tailed-PCR-based mapping library using slightly different methods. The *LUC* loci obtained were combined in the final step.

(D)

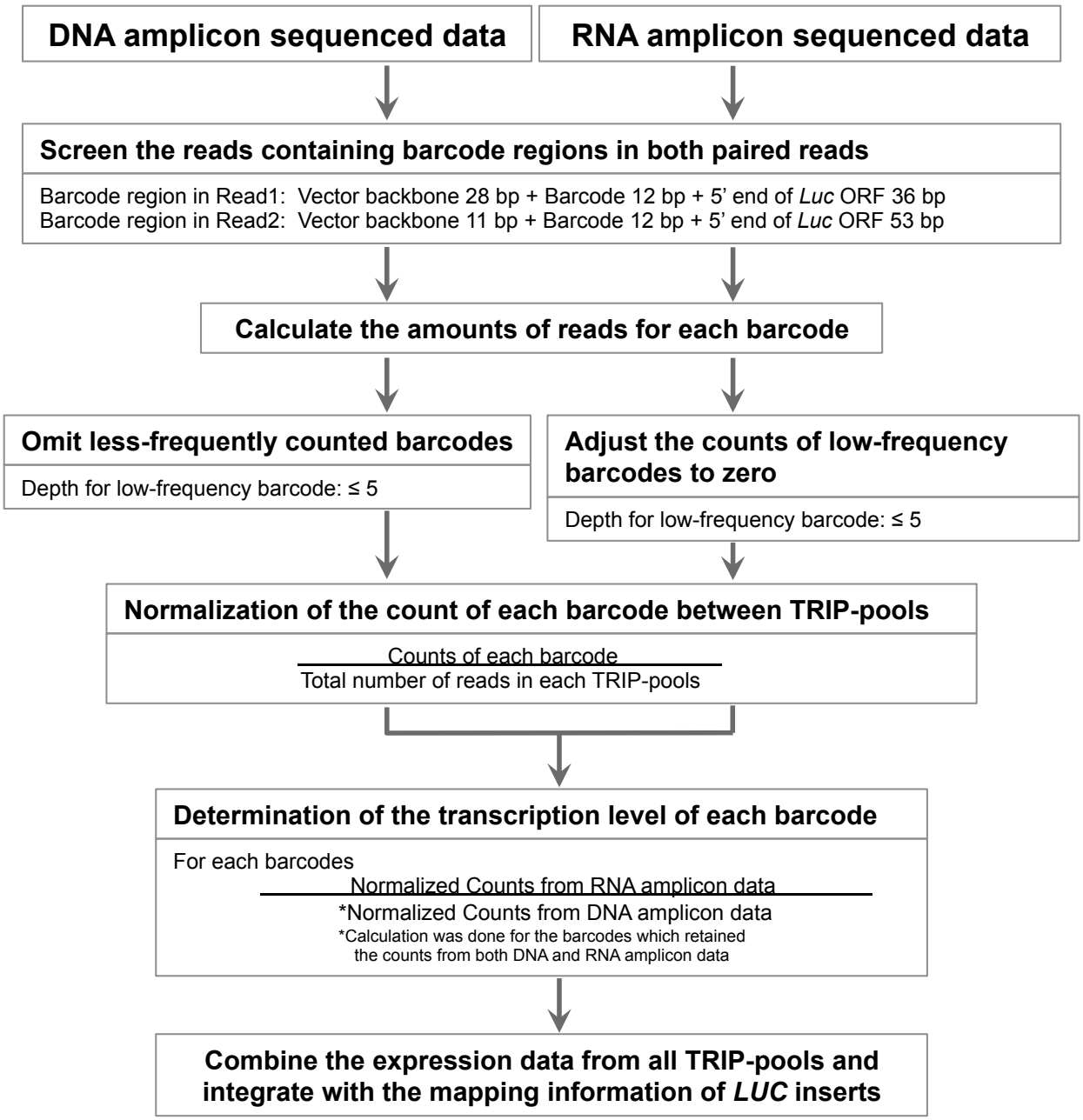

S1 Fig. Precise workflow of the promoter analysis that was performed using the TRIP system. (D) Flow diagram used for the determination of *LUC* transcription levels. The transcription level data obtained for individual barcodes were associated with the respective mapped *LUC* genes and used in subsequent analyses.

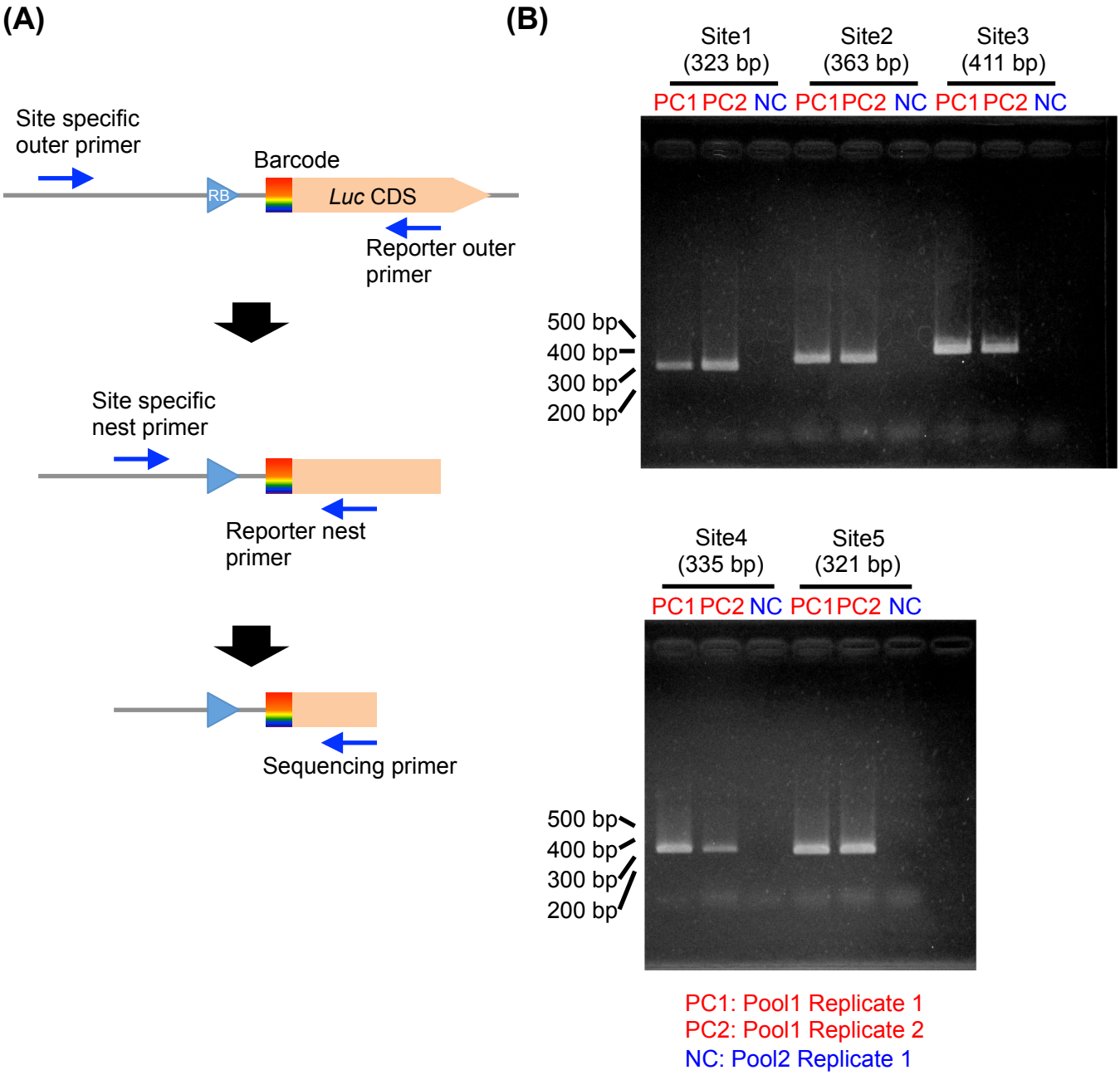

S2 Fig. Validation of the *LUC* mapped loci and barcode sequences via PCR amplification in five representative samples. (A) Schematic diagram of the nested PCR that was performed using insertion-site-specific and *LUC*-specific primers. (B) Five *LUC* genes were chosen from the TRIP-Pool1 and detected by PCR. PC1 and PC2 are technical replicates of the PCR using the template DNA from TRIP-Pool1 cells. NC is the PCR product from the DNA of TRIP-Pool2 and was used as a negative control. The PCR products were loaded onto a 2% agarose gel. The expected size of the PCR products is shown at the top of the gel, in parentheses. The PCR products obtained were Sanger sequenced for verification of the barcode sequences.

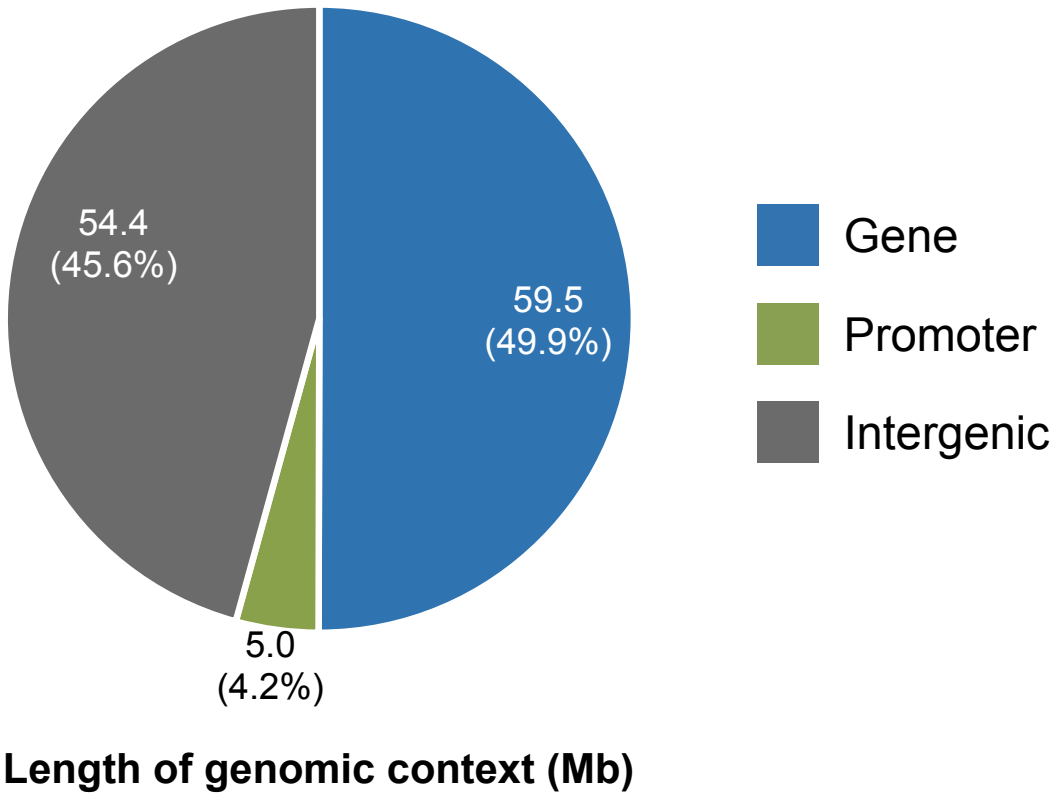

S3 Fig. Length of each genomic context. The total length of the respective genomic contexts and their percentage in the whole genome are shown. The 200 bp segments 5′-proximal to the genic region (CDS plus UTR regions according to TAIR10) were defined as promoter regions, and the remaining sequences were defined as intergenic regions. When neighboring promoter and genic regions were overlapped, those parts were omitted from the statistical analyses described above (their sum was 0.23 Mb, 0.2% of the whole genome).

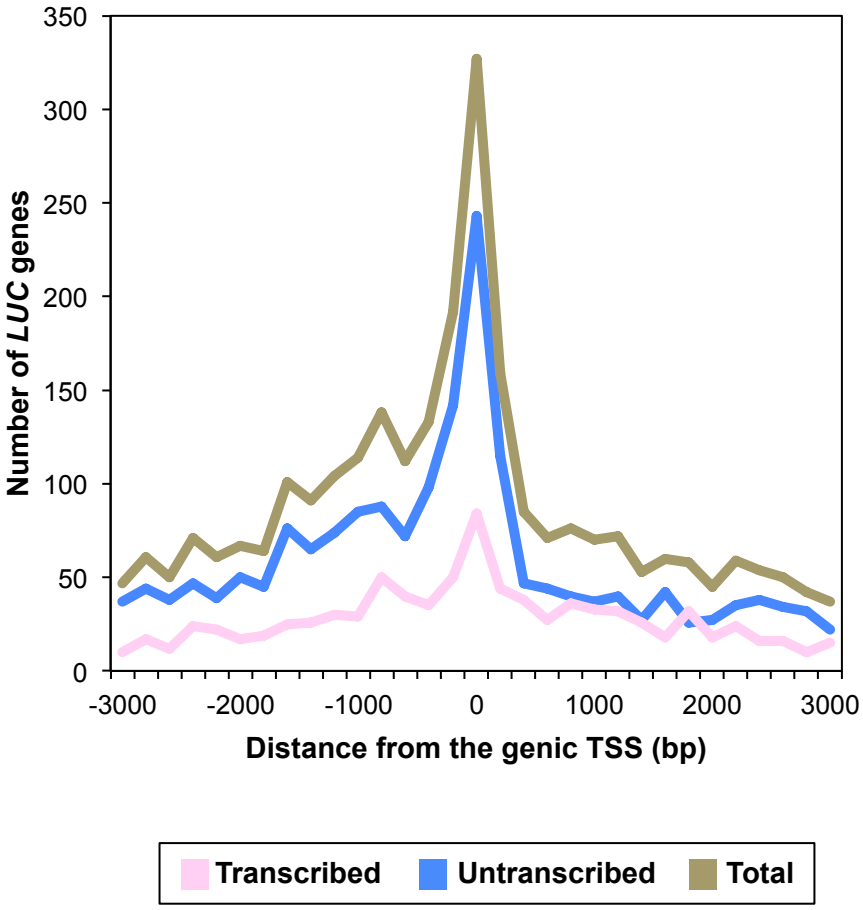

S4 Fig. Abundances of *LUC* genes relative to the nearest genic TSS. Number of LUC genes in relation to the distances from the genic TSS was counted in 200 bp window size.

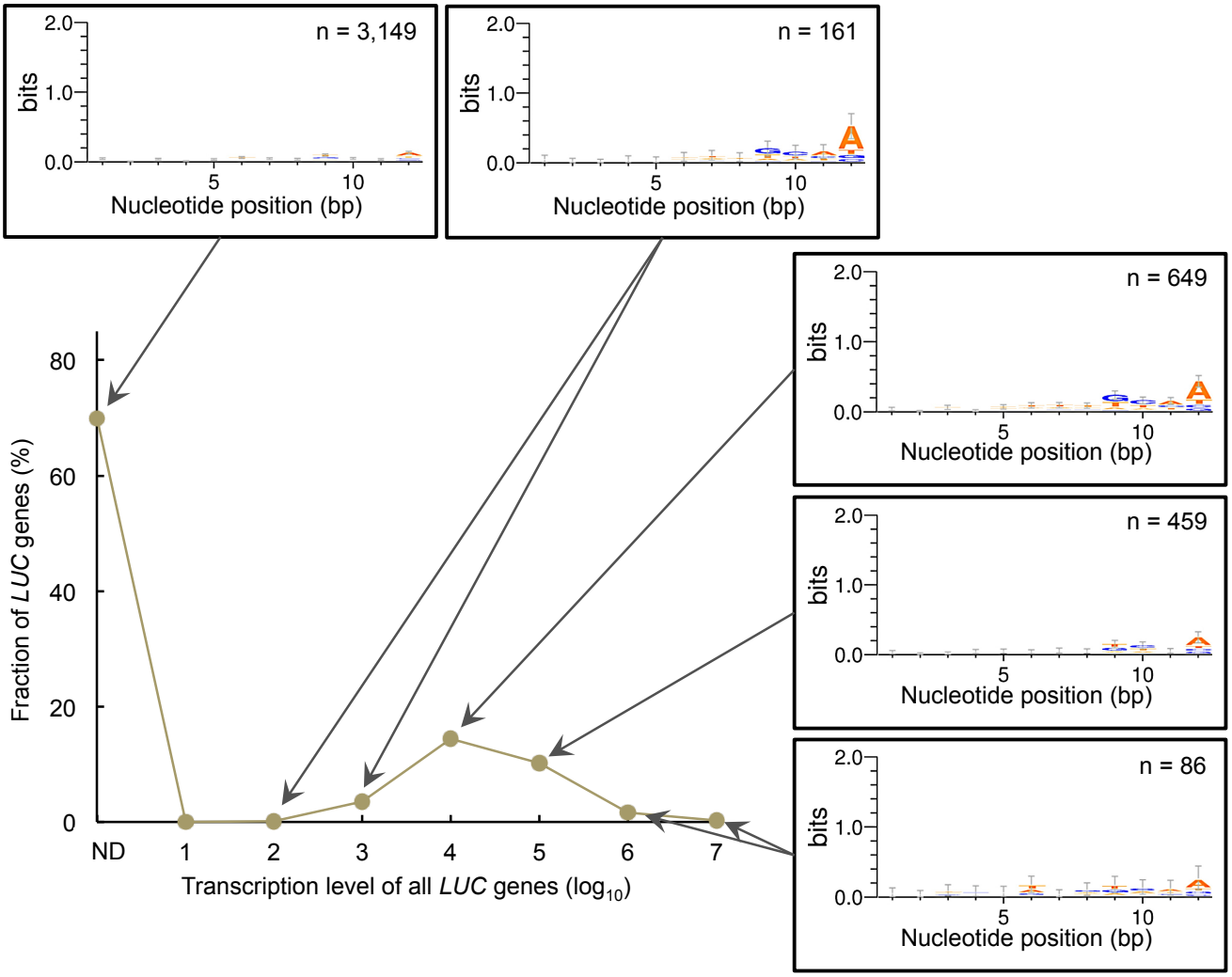

S5 Fig. Assessment of the effect of barcode sequences on the LUC transcription levels. Frequently observed barcode motifs in the LUC insert of indicated transcription levels were analyzed using WebLogo3 (Crooks *et al.*, 2004). The transcription levels of all the LUC genes are shown as in Fig 1D. A weak positional preference for 'A' was found at the 3′-terminal position on the barcode. However, the frequency of 'A' at this position did not correlate with the strength of transcription.

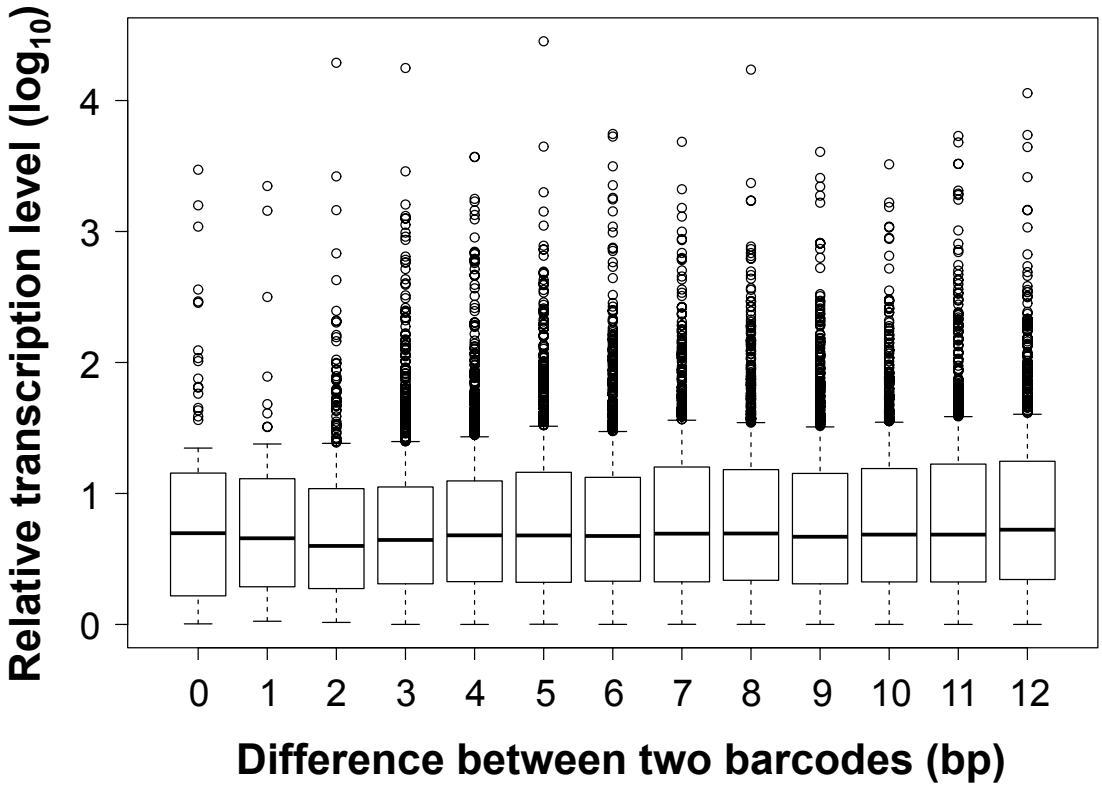

S6 Fig. Similarity/dissimilarity of the transcription levels of the randomly selected LUC pairs against the sequence identity of the 12-base barcode. A pair of LUC genes was randomly selected from the 4,504 mapped LUC genes, and the similarity/dissimilarity of their transcription levels is shown as the ratio of their RNA levels in a logarithmic scale; the ratio was calculated by dividing the higher RNA level by the lower level (i.e., log(ratio) ≥0). The similarity/diversity of the barcode is indicated by the number of mismatched nucleotides at the corresponding positions. This graph is the summary of the analysis of 10,566 LUC pairs and indicates the absence of a correlation between the similarity of the barcode sequence and that of the transcription level. In other words, the barcode sequence does not affect the transcription level of LUC genes.

Methods note: 1) When randomly selected LUC pairs were located within 100 kb on the same chromosome, they were omitted from the analysis, lest their positional effect should influence their transcription levels. 2) One thousand LUC pairs were analyzed each for the indicated number of mismatches in the barcode. However, for mismatch numbers of 0, 1, and 2, the number of LUC pairs analyzed was 92, 51, and 423, respectively. This is because the number of such highly homologous barcodes in the total population of 4,504 LUC inserts was limited, and these are all the LUC genes that fulfilled the given requests. 3) The LUC inserts of the identical barcodes were derived from different TRIP pools, because LUC mapping in a given TRIP pool had been conducted so that the individual LUC genes were mapped to a unique locus, with omission of those that were mapped to more than one locus.

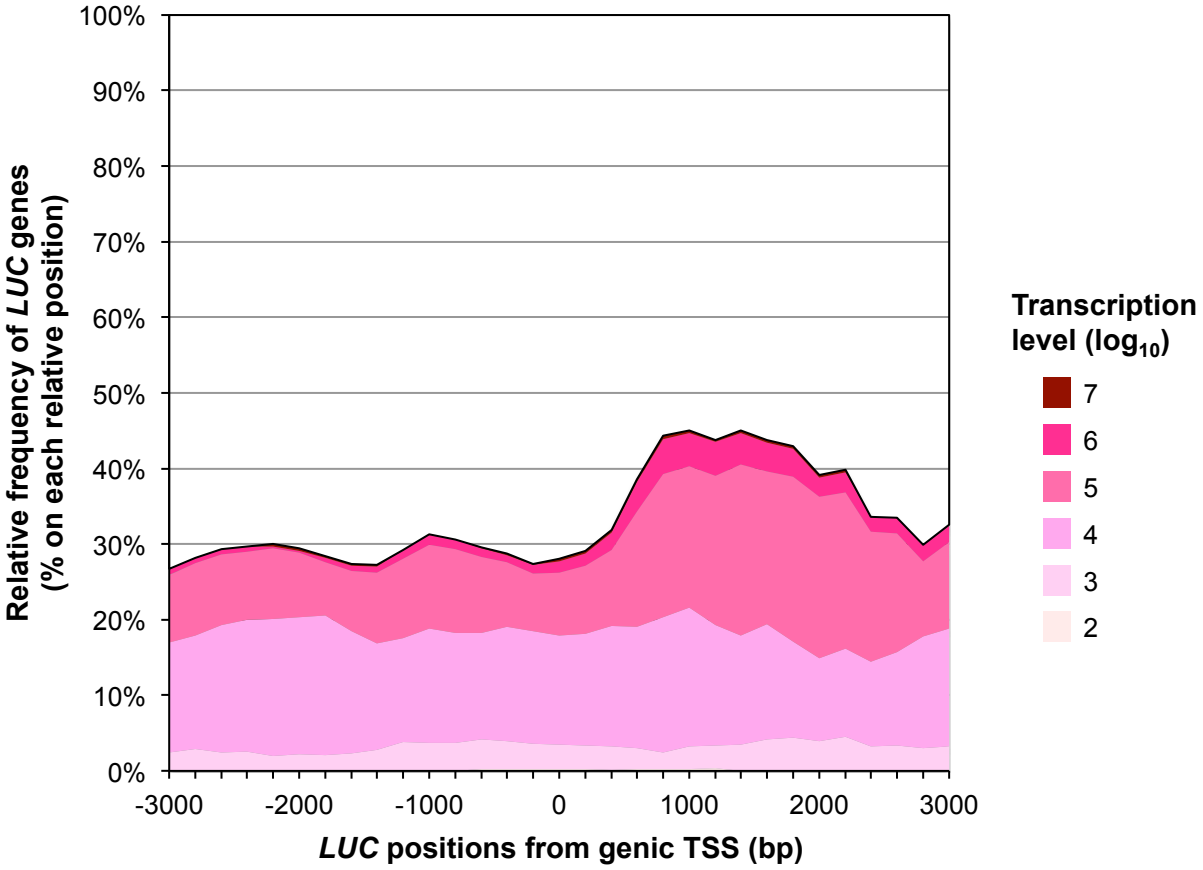

S7 Fig. Frequency of transcribed *LUC* genes relative to the annotated genic TSS. Abundance of the *LUC* genes with the indicated transcription levels in relation to the distance from the genic TSS, as shown in Fig 1E. The plot was smoothed by calculating the five-point moving average of integration frequency in each window (200 bp).

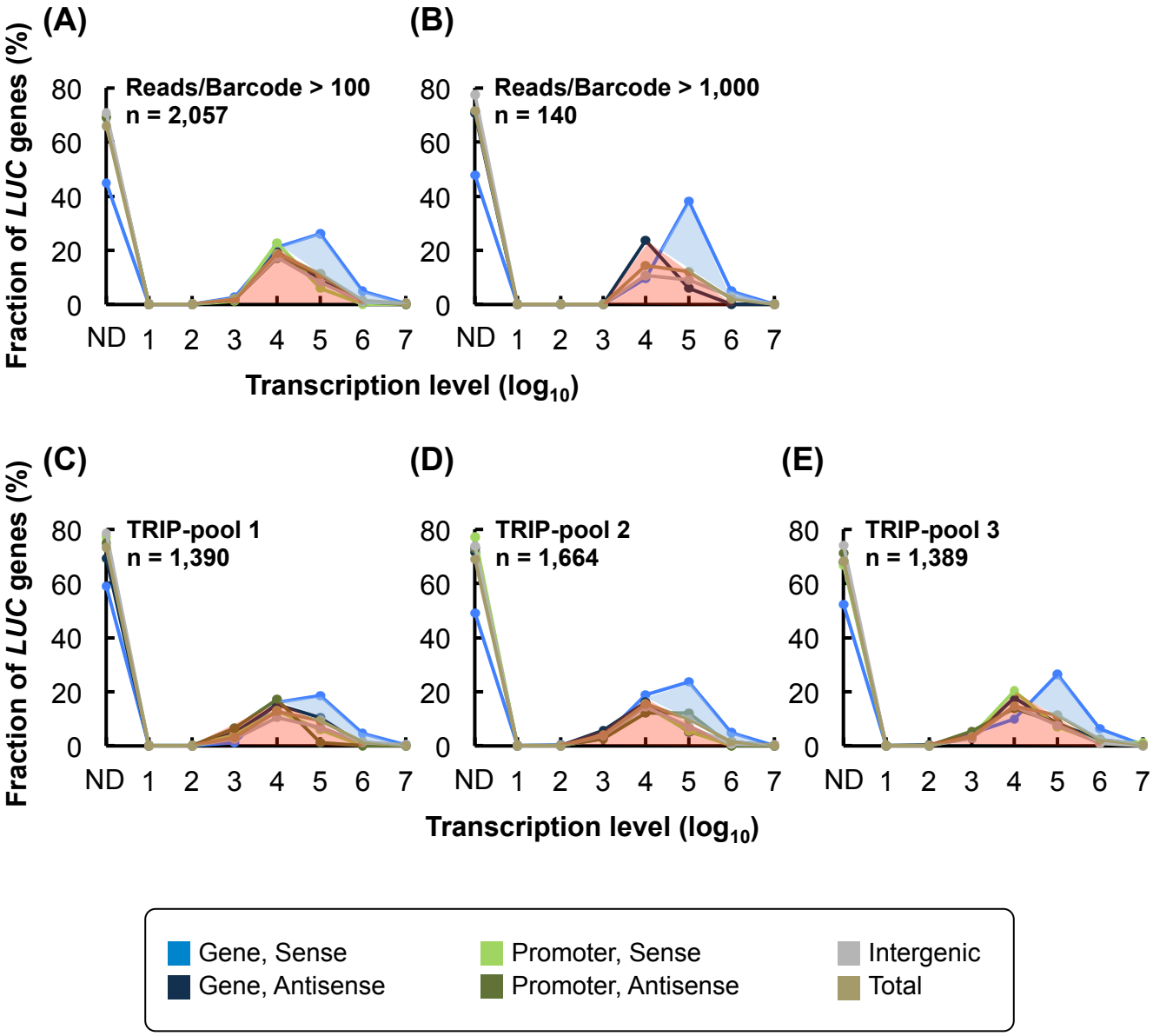

S8 Fig. Expression profiles of LUC genes with high-number reads from the amplicon-sequencing data and of LUC genes from biological replicates. (A and B) For each barcode, when the number of reads from DNA amplicon sequencing was up to (A) 100 or (B) 1,000, the barcode was omitted from the analysis. The number of reads for each barcode obtained from RNA amplicon sequencing was redefined as zero, if the number of reads was below such thresholds. The subsequent processes used in this analysis were same as those used in Fig 1D. The expression profiles of the LUC genes located in promoter regions were omitted from (B), because the number of such LUC genes was insufficient to represent their profiles. (C–E) Expression profiles of three biological replicates. The numbers of LUC genes shown in all graphs are the total amount of LUC genes used for their analysis. The fraction of the transcribed *LUC* genes attributed by two distinct mechanisms are indicated by light-blue and light-red areas.

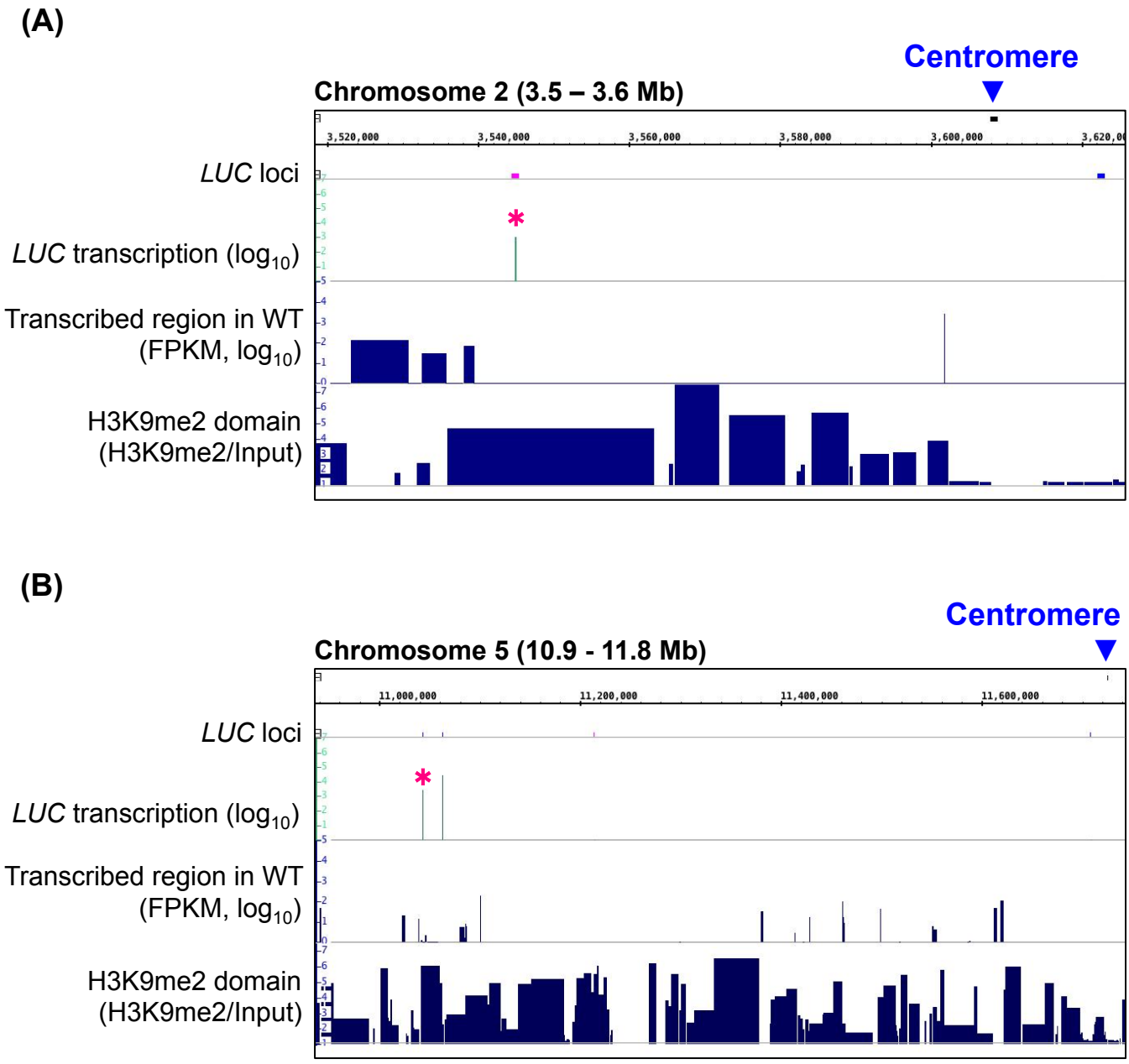

S9 Fig. Two examples of transcribed LUC genes in the H3K9me2-marked regions located around the centromere. (A and B) Transcribed LUC genes (asterisk) were found 63 kb and 682 kb away from the centromeres of chromosomes 2 (A) and 5 (B), respectively. The respective H3K9me2 levels of these loci were 80 (A) and 91 (B) percentiles, respectively. In WT T87 cells, transcripts were very scarce in these heterochromatic regions.

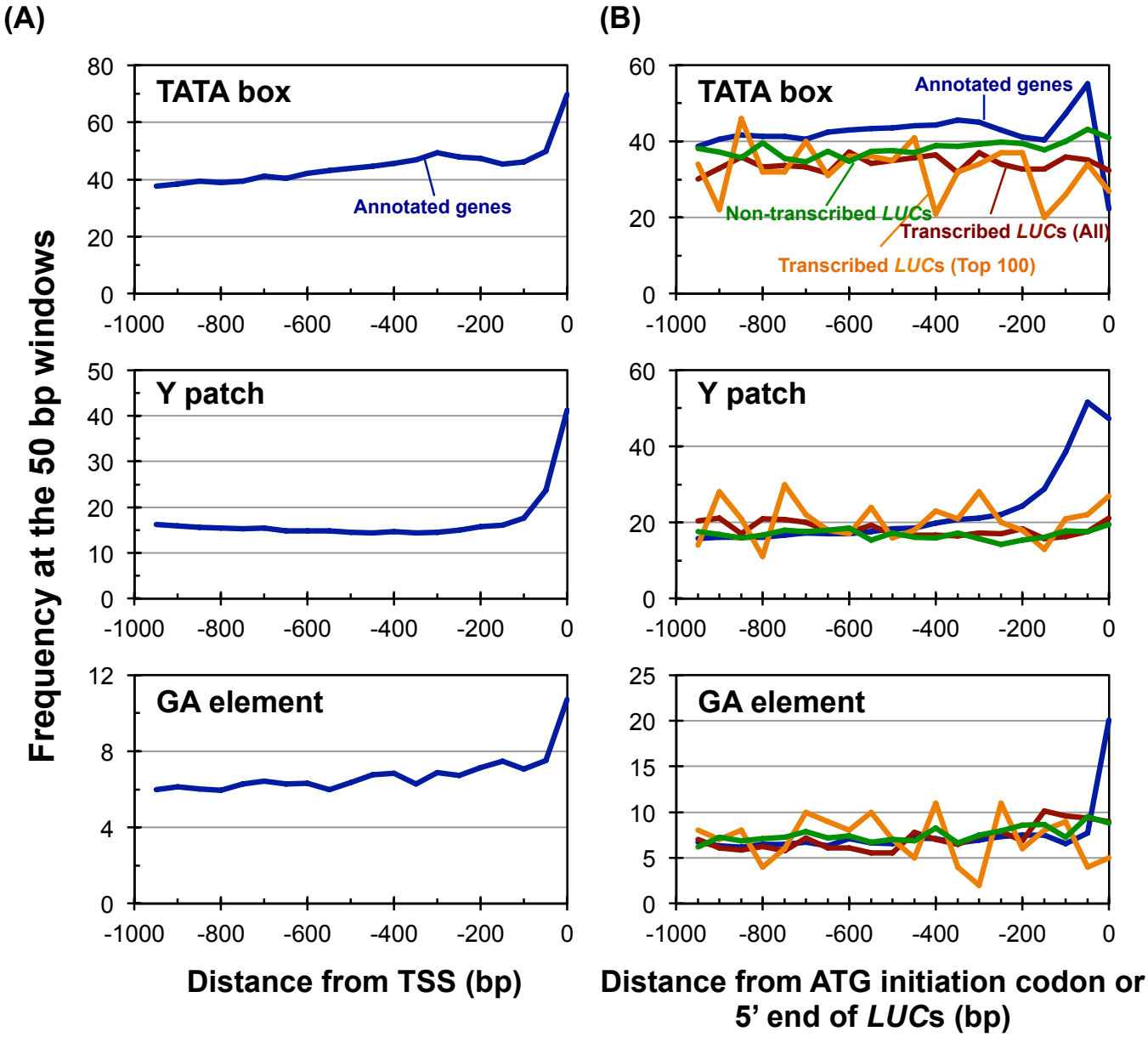

S10 Fig. Distribution of *cis*-regulatory elements in the upstream region of *LUC* integration sites. (A and B) The frequency of TATA-box, Y patch, and GA elements in the upstream region of the (A) TSS of annotated genes, or (B) of ATG initiation codons of annotated genes and 5′ ends of *LUC* inserts were analyzed according to Yamamoto *et al.* (Yamamoto *et al.*, 2007) using a window size of 50 bp for the high-sensitive detection of the motifs. The Y-axis represents the fraction of genes or *LUC* genes that contained the indicated motifs.

S1 Table. Primer list

T-DNA library construction

Name	Sequence (5' -> 3')	Descriptions
TRIP_LUC_EcoRI_r	TTAGGTAACCCAGTAGATCCAGAGG	These primers were used to introduce barcode into the T-DNA. Barcode was indicated by n.
TRIP_ITLB_barcodeF	AAAGTCGACGTTATCAGCTTACAGnnnnnnnnnnnnATGGAAGACGCCAAAAACAT	

Sequencing library preparation for the locus determination (TAILed-PCR based)

Name	Sequence (5' -> 3')	Descriptions
TRIP_LUC_iPCR_F1.1	GTTGGGCGCGTTATTTATCGGAGTT	Primer set for the inverse PCR to specifically amplify *LUC*-including DNAs.
TRIP_LUC_iPCR_R1	GTTTTCACTGCATACGACGATTCTG	
TRIP_iPCRAmpSeq_F2.1	gtctcgtgggctcggagatgtgtataagagacagCACATCTCATCTACCTCCCGGTTT	Primer set for the TAILed-PCR following the inverse PCR in order to add adapter sequence for next-generation sequencing. Adapter sequences were lowercased.
TRIP_iPCRAmpSeq_R2.1	tcgtcggcagcgtcagatgtgtataagagacagCTCTAGAGGATAGAATGGCGCCG	

Sequencing library preparation for the locus determination (Nextera based)

Name	Sequence (5' -> 3')	Descriptions
TRIP_LUC_iPCR_F1.1	GTTGGGCGCGTTATTTATCGGAGTT	Primer set for the inverse PCR to specifically amplify *LUC*-including DNAs.
TRIP_LUC_iPCR_R1	GTTTTCACTGCATACGACGATTCTG	
TRIP_LUC_iPCR_F2.1	CATTTCGCAGCCTACCGTAGTGTTT	Primer set for the nested-PCR following inverse PCR to specifically amplify *LUC*-including DNAs.
TRIP_LUC_iPCR_R2.2	CATTTCGAAGTATTCCGCGTACGTG	

Sequencing library preparation for the transcription level analysis

Name	Sequence (5' -> 3')	Descriptions
TRIP_AmpSeq_F_New2	tcgtcggcagcgtcagatgtgtataagagacagTCAAGGCCTCGACGTTATCAGC	Primer set for amplyfing barcode region of cDNA/DNA with adding adapter sequence for next-generation sequencing. Adapter sequences were lowercased.
TRIP_AmpSeq_R	gtctcgtgggctcggagatgtgtataagagacagTCTAGAGGATAGAATGGCGCCGG	

Primer sets for validation of *LUC* mapped loci and barcode

Name	Sequence (5' -> 3')	Descriptions
TRIP_LUC_iPCR_R1	GTTTTCACTGCATACGACGATTCTG	Reporter outer primer (see Supplementary Figure S2).
TRIP_LUC_iPCR_R2.2	CATTTCGAAGTATTCCGCGTACGTG	Reporter nest primer (see Supplementary Figure S2).
C1_CGGAAAGACCAA_AS_F1	TCCTCAATGAGTCTGGTGACTTC	Site1 specific outer primer (see Supplementary Figure S2).
C1_CGGAAAGACCAA_AS_F2	CTCATTGCCCTCAGGTTGGT	Site1 specific nest primer (see Supplementary Figure S2).
C2_GCACAAAGTCTA_S_F1	TCACTGCTCAATGCGATCTCC	Site2 specific outer primer (see Supplementary Figure S2).
C2_GCACAAAGTCTA_S_F2	TTAGTGTCGCAACAACGAACCG	Site2 specific nest primer (see Supplementary Figure S2).
C3_CTAGGGGACTCA_AS_F1	TTCGATCCTTCAAAGCGCATCAC	Site3 specific outer primer (see Supplementary Figure S2).
C3_CTAGGGGACTCA_AS_F2	CAAGGAGCTTGTCTGGAGAGAG	Site3 specific nest primer (see Supplementary Figure S2).
N1_TGATGATGTCCA_S_F1	GACTACAAATCATTCATCAACCACG	Site4 specific outer primer (see Supplementary Figure S2).
N1_TGATGATGTCCA_S_F2	TAGTTGATTCCTCTCGTTCGGC	Site4 specific nest primer (see Supplementary Figure S2).
T1_TTAGTTGGTCAA_AS_F1	CCAATCTGACACAAAATAGGTCTCT	Site5 specific outer primer (see Supplementary Figure S2).
T1_TTAGTTGGTCAA_AS_F2	TTAAAGAGGAGTCACGATCATCGGT	Site5 specific nest primer (see Supplementary Figure S2).

H3K9me2 ChIP validation

Name	Sequence (5' -> 3')	Descriptions
55670F1	CGTTGCTGACGACGGGTTTATGG	Primer set for validation of H3K9me2-ChIP according to To et al., 2011.
55670R1	GTTTCTAGATCCCGCTTCGTCGTTC	
63935F1	CGTTGTAGGTCAGGGTTCTTGC	Primer set for validation of H3K9me2-ChIP according to To et al., 2011.
63935R1	GCCATAGATGCATCACGAACCG	
44070F1	ACTTCCTCGACCTCTTATCTCC	Primer set for validation of H3K9me2-ChIP according to To et al., 2011.
44070R1	CTTCGGTTTAACCCAGAGAGATG	
ACT2F2	GATCTCCAAGGCCGAGTATGAT	Primer set for validation of H3K9me2-ChIP according to To et al., 2011.
ACT2R2	CCCATTCATAAAACCCCAGC	
67105F1	TGTCTCCAGTTTGATCCGGATTTG	Primer set for validation of H3K9me2-ChIP according to To et al., 2011.
67105R1	GTAACAGAAGATCCGATATGTAATCGG	
G683F1	TCCGATCTGAGATCGGTAGCCG	Primer set for validation of H3K9me2-ChIP according to To et al., 2011.
G683R1	CGAAACAAACCCACGACACTCC	